

IGNITION CHARACTERISTICS OF A COMBUSTIBLE MIXTURE  
IN OPPOSED FLOW WITH A HOT INERT GAS

A THESIS

Presented to  
The Faculty of the Division  
of Graduate Studies

By  
Heng-wai Hsu

In Partial Fulfillment  
of the Requirements for the Degree  
Doctor of Philosophy  
in the School of Mechanical Engineering

Georgia Institute of Technology

April, 1976

# IGNITION CHARACTERISTICS OF A COMBUSTIBLE MIXTURE

IN OPPOSED FLOW WITH A HOT INERT GAS

Approved:

P. Durbetaki, Chairman

~~M. R. Corley~~ 0

S. P. Kezios

E. A.<sup>o</sup> Powell

~~H. C. Ward~~

Date approved by Chairman: 4/14/1976

## ACKNOWLEDGMENTS

The author is indebted to the individuals who have contributed to the success of this work. In particular, he would like to express his appreciation to his thesis advisor, Dr. P. Durbetaki, for his valuable assistance. He would also like to thank Drs. M. R. Corley, S. P. Kezios, E. A. Powell, and H. C. Ward, who served as members of the thesis reading committee.

The author would like to express his sincere appreciation to his parents for their loving guidance and to his wife for her love, patience and understanding.

## TABLE OF CONTENTS

	Page
ACKNOWLEDGMENTS. . . . .	ii
LIST OF TABLES . . . . .	v
LIST OF ILLUSTRATIONS. . . . .	vi
NOMENCLATURE . . . . .	viii
SUMMARY. . . . .	xii
Chapter	
I. INTRODUCTION. . . . .	1
1.1. Relevance of the Problem	
1.2. Objectives of the Dissertation	
II. LITERATURE REVIEW . . . . .	5
III. ANALYSIS. . . . .	12
3.1. Formulation of the Problem	
3.1.1. General Formulation of the Problem	
3.1.2. General Formulation	
3.1.2.1. Conservation Equations	
3.1.2.2. Constitutive Equations	
3.1.3. Boundary Layer Equations	
3.1.4. Boundary Conditions	
3.1.4.1. The Impinging Jet	
3.1.4.2. The Opposed-Jet	
3.2. Similarity Transformation	
3.2.1. Similarity Groups and Trans-	
formation	
3.2.1.1. Purpose of the Trans-	
formation	
3.2.1.2. General Techniques of	
Transformation	
3.2.2. Transformation of the Governing	
Equations	
3.2.3. The Stoichiometry Measure	
3.2.4. Boundary Conditions	
3.2.4.1. The Impinging Jet Case	
3.2.4.2. The Opposed-Jet Case	



Chapter	Page
IV. METHOD OF SOLUTION. . . . .	36
4.1. Further Simplification of the Governing Equations	
4.2. Method of Solution	
4.3. The Impinging Jet Solution	
4.3.1. The Boundary Conditions	
4.3.2. The Procedure of Solution	
4.4. The Opposed-Jet Solution	
4.4.1. The Boundary Conditions	
4.4.2. Procedure of Solution	
4.5. Specification of Parameters	
4.6. Numerical Method	
4.6.1. Introduction	
4.6.2. Discussion of the Method	
V. RESULTS AND DISCUSSION. . . . .	46
5.1. Results of the Impinging Jet	
5.1.1. Fuel Mass Fraction at the Wall	
5.1.2. Dependence of Skin Friction on $\bar{D}_I$	
5.1.3. Heat Transfer Rate Dependence on $\bar{D}_I$	
5.1.4. Velocity Distribution	
5.1.5. Fuel Concentration Profiles	
5.1.6. Temperature Distribution	
5.1.7. Heat Transfer Rate Dependence on $f_w$	
5.1.8. Dependence of $\bar{D}_{I,i}$ on $f_w$	
5.2. Results of the Opposed-Jet Case	
5.2.1. Ignition Characteristics	
5.2.2. Velocity Distribution	
5.2.3. Fuel Concentration Profiles	
5.2.4. Temperature Distribution	
5.3. Generalized Ignition-Extinction Characteristics	
VI. CONCLUSIONS . . . . .	72
VII. RECOMMENDATIONS . . . . .	74
REFERENCES . . . . .	75
OTHER REFERENCES . . . . .	78
VITA . . . . .	79

## LIST OF TABLES

Table		Page
1.	Values for Constant $a$ . . . . .	28
2.	Critical Damköhler Numbers at Different $f_w$ . . .	61

## LIST OF ILLUSTRATIONS

Figure		Page
1.	Coordinate System of an Impinging Jet. . . . .	13
2.	Coordinate System of Opposed-Jet . . . . .	14
3.	The Fuel Concentration at the Interface as Function of the First Damköhler Number with Inert Gas Injection Rate as a Parameter, $\theta_w = 3.0$ . . . . .	48
4.	Dependence of the Skin Friction on the First Damköhler Number with Inert Gas Injection Rate as a Parameter, $\theta_w = 3.0$ . . . . .	50
5.	Dependence of Surface Heat Transfer Rate on the First Damköhler Number with Inert Gas Injection Rate as a Parameter, $\theta_w = 3.0$ . . . . .	51
6.	Comparison of Velocity Profiles at Specified Damköhler Numbers and Inert Gas Injection Rates. . . . .	53
7.	Comparison of Fuel Concentration Profiles at Specified Inert Gas Injection Rates. . . . .	55
8.	Comparison of Temperature Profiles at Specified Damköhler Numbers and Inert Gas Injection Rates. . . . .	57
9.	The Effect of Inert Gas Injection on the Surface Heat Transfer. . . . .	58
10.	The Effect of Inert Gas Injection on the Ignition First Damköhler Number in the Impinging Jet. . . . .	60
11.	Dependence of Maximum Temperature on the First Damköhler Number in the Opposed-Jet Case, $\theta_{-\infty} = 3.0$ . . . . .	62
12.	Comparison of Velocity Profiles at Specified Damköhler Numbers in the Opposed-Jet Case, $\theta_{-\infty} = 3.0$ . . . . .	64
13.	Comparison of Fuel Concentration Profiles at Specified Damköhler Numbers in the Opposed-Jet Case, $\theta_{-\infty} = 3.0$ . . . . .	66

Figure	Page
14. Comparison of Temperature Profiles at Specified Damköhler Numbers in the Opposed-Jet Case, $\theta_{-\infty} = 3.0$ . . . . .	68
15. Ignition and Extinction Characteristics of a Stagnation Point Flow. . . . .	70

## NOMENCLATURE

## Symbols

$a$	coefficient of the potential velocity
$B$	overall frequency factor
$C$	$\rho\mu/\rho_e\mu_e$
$C_p$	specific heat at constant pressure
$D$	mass diffusivity
$D_I$	Damköhler's first dimensionless group, $B\rho_e/a$
$\bar{D}_I$	first Damköhler number, $\frac{1}{2} \nu_0 W_0 Y_{F,e} D_I$
$\bar{D}_{I,e}$	critical first Damköhler number for extinction
$\bar{D}_{I,i}$	critical first Damköhler number for ignition
$D_{II}$	Damköhler's second dimensionless group, $q^0/C_{p,e} T_e$
$\bar{D}_{II}$	second Damköhler number, $Y_{F,e} D_{II}$
$D_T$	thermal diffusion coefficient
$E$	activation energy
$E^*$	dimensionless activation energy, $E/RT_e$
$\tilde{f}_i$	external force per unit mass on species $i$
$f'(\eta)$	dimensionless velocity, $u/u_e$
$h_i$	specific enthalpy of species $i$
$h_i^0$	standard heat of formation per unit mass for species $i$ at temperature $T_0$
$k$	thermal conductivity
$\ell$	bulk viscosity coefficient
$Le$	Lewis number, $\rho_e D C_{p,e}/k_e$

$m$	constant for variable $\xi$
$M$	total number of chemical reactions occurring
$N$	total number of chemical species present
$n_e$	dimensionless "stoichiometry" measure
$Nu$	Nusselt number, $q_w x / k_w (T_e - T_w)$
$p$	hydrostatic pressure
$\bar{p}$	pressure tensor
$Pr$	Prandtl number, $C_{p,e} \mu_e / k_e$
$q^o$	standard heat of reaction
$\vec{q}$	heat flux
$\gamma_o$	cylindrical radius of surface
$R$	universal gas constant
$Re$	Reynolds number, $u_e x \rho_e / \mu_e$
$s$	$\int_0^x \rho_e \mu_e u_e r_o^2 dx$
$Sc$	Schmidt number, $\mu_e / \rho_e D$
$t$	time
$T$	temperature
$u, v$	velocity coordinates
$U$	specific interval energy of the gas mixture
$U_\infty, U_{-\infty}$	jet velocities of the opposed-jet
$\bar{U}$	unit tensor
$\vec{V}_i$	diffusion velocity of species $i$
$\vec{v}$	mass-average velocity of species
$w_i$	rate of production of species $i$ by chemical reactions
$W_i$	molecular weight of species $i$



$x$	distance along surface
$X_i$	mole fraction of species $i$
$y$	distance normal to surface
$Y_i$	mass fraction of species $i$
$\alpha_i$	dimensionless mass fraction of species $i$ , $Y_i/Y_{i,e}$
$\alpha_k$	exponent determining the temperature dependence of the frequency factor for the $k^{\text{th}}$ reaction
$\zeta$	assumed values of initial conditions
$\eta$	$(\rho_e \mu_e r_o)/(2s)^{1/2} \int_0^y (\rho/\rho_e) dy$
$\theta$	dimensionless temperature, $T/T_e$
$\mu$	viscosity
$\nu$	stoichiometric coefficient
$\nu'_{i,k}$	stoichiometric coefficient of species $i$ appearing as a reactant in reaction $k$
$\nu''_{i,k}$	stoichiometric coefficient of species $i$ appearing as a product in reaction $k$
$\xi$	$\rho_e \mu_e a x^{2(m+1)}/2(m+1)$
$\rho$	density
$\psi$	stream function
$\omega$	reaction rate of combustible component
Subscript	
$e$	at the boundary of the boundary layer in the impinging jet case or at the boundary of the boundary layer of the combustible mixture side in the opposed-jet case
$e-$	at the boundary of the boundary layer of the inert gas side in the opposed-jet case
$F$	fuel

i	$i^{\text{th}}$ species
N	inert gas
O	oxidizer
P	product
w	at the surface
$\infty$	free stream at the combustible mixture side
$-\infty$	free stream at the inert gas side



## SUMMARY

The ignition characteristics of a combustible mixture in opposed flow with a hot inert gas have been considered. Two cases were studied: (i) a jet of a combustible mixture impinging on a blunt body with hot inert gas injection from the wall near the stagnation point, and (ii) an opposed jet of a premixed combustible mixture and a hot inert gas, respectively. The flow has been considered to be compressible. The injection rate in case (i) and the temperature of the inert gas jet in case (ii) are the main factors which affect the combustion characteristics. A critical first Damköhler number has been found beyond which no ignition is possible.

The Newton-Raphson and the least-square methods have been used to find the initial conditions that will enable the solution to satisfy the asymptotic conditions at the edge of the boundary layer. The method is effective, fast converging, and it can be employed to solve problems of similar type.

The results show that with higher injection rate of inert gas, the ignition of the premixed combustible mixture is delayed. The first Damköhler number of ignition increases linearly with the inert gas injection rate. In the opposed-jet case, the relationship between the maximum temperature in the flow field and its corresponding Damköhler number gives a characteristic curve of opposed-jet combustion.

## CHAPTER I

### INTRODUCTION

#### 1.1. Relevance of the Problem

The problem of ignition and extinction in forced convection systems is of considerable interest. The ignition of gaseous mixtures is considered one of the important phenomena in the field of combustion. It is the process by which a propagating flame originates in the mixture. Its importance was recognized quite early, and analytical and experimental work was undertaken by combustion researchers in order to shed some light on its complex mechanisms and the factors affecting them. Various methods have been used by which combustible gaseous mixtures have been ignited. Heated surfaces and hot gases are just two of these methods.

Several studies have been made during the last three decades on the heat interaction between reactive mixtures of gases and solid surfaces. The research was also extended to the study of the opposed flow of two streams. Interest in these problems was instigated by the need to understand phenomena relating to hypersonic flight in air, thermal protection of re-entry vehicles by heat shields and ablating surfaces, flame stabilization by solid surfaces, burning of liquid fuel or solid fuel surfaces in a flowing oxidizing

atmosphere, as well as, ignition and extinction characteristics of premixed and unmixed combustible flowing gases. All these problems are concerned with reactive processes in the boundary layer and a class of these problems is associated with the heat interaction between a reactive mixture of gases and hot solid surfaces (or hot gas stream), at the stagnation region.

The early research on stagnation flows was related to the study of laminar heat-transfer in the dissociated boundary layer of air at the stagnation region [1,2]. The ignition and extinction problem of initially unmixed reactants in an opposed flow configuration was considered by Fendell [3] and his analysis demonstrated the multi-valued transition from frozen to equilibrium flow. The heat interaction between a premixed combustible mixture and a hot surface at the stagnation region has also been investigated. These studies have been carried out to consider the effect of the hot surface on the ignition and extinction characteristics of the mixture.

Some of the studies on the ignition and extinction characteristics of a combustible mixture [4-7] utilized the Van's Hoff critical ignition condition, which states that a combustible mixture near the non-catalytic surface of a body will ignite when the temperature gradient normal to the wall is zero. All of these assumed incompressible flow for the fluid. The analysis has also been made by examining the steady-state solution of the conservation equations in the



region comprising the transition of frozen to equilibrium flow, without the use of the Van's Hoff criterion [8], and without the assumption of incompressible flow [9,10].

The present work investigates the heat interaction of a cold combustible mixture with a hot inert gas injected both through the porous wall and in free opposed flow. The ignition of the cold combustible mixture is also studied. The fluid is considered to be compressible. The injection rate of the hot inert gas and the temperature of the hot inert gas stream are varied to establish their effect on the ignition and flow parameters.

### 1.2. Objectives of the Dissertation

As mentioned in the previous section, the problem of stagnation-point and opposed-jet combustion has been investigated by some researchers in the last three decades. Due to the complex nature of the problem, most of this work has been carried out by assuming incompressible flow to simplify the problem by uncoupling the energy and species conservation equations from the momentum conservation equation [3,11,12,13]. Alkidas and Durbetaki [9] and Smith, et al. [10] were the first ones to include compressibility in their analysis to obtain a more exact solution. However, there has been no attempt to study the interface heat transfer and ignition characteristics of a premixed combustible mixture with a hot inert gas in opposed flow. With hot inert gas injected from

the wall near the stagnation region of a blunt body and especially in the opposed jet flow configuration the complexity of the problem increases and an efficient method must be developed to achieve a solution of the problem.

The objectives of the present dissertation are as follows:

(1) To formulate the interaction of a hot inert gas with a cold premixed combustible mixture in opposed flow and establish the conditions of ignition.

(2) To relax the assumption of incompressible flow and solve the governing equations for the compressible fluid.

(3) To develop a numerical technique to solve the coupled system of equations with the associated boundary conditions.

## CHAPTER II

### LITERATURE REVIEW

The earliest accurate analysis related to reacting boundary layers appeared in the literature about two decades ago. Von Karman and Millan [14] using boundary-layer analysis considered the quenching effect of the cold wall downstream from a premixed laminar flame. Marble and Adamson [15] investigated the ignition of a premixed combustible gas by a hot inert gas stream flowing in parallel and mixing with the combustible gas. Emmons [16] studied the burning of a semi-infinite flat plate of solid or liquid fuel placed parallel to a flowing oxidizing stream. The fuel was maintained at a constant temperature.

The study of laminar heat-transfer in the dissociated boundary layer of air at the stagnation region represents some of the early investigations on stagnation flow. Lees [1] dealt with two limiting cases of laminar heat transfer over blunt-nosed bodies at hypersonic flight speeds, or high stagnation temperature: (a) thermodynamic equilibrium, in which the chemical reaction rates are regarded as "very fast" compared to the rates of diffusion across streamlines, and (b) diffusion is rate governing, in which the volume recombination rates within the boundary layer are "very slow"

compared to diffusion across streamlines. Fay and Riddell [2] developed the boundary-layer equations for the case of very high speed flight where the external flow is in a dissociated state. In particular the effects of diffusion and of atom recombination in the boundary-layer were included. For the non-equilibrium boundary layer, both catalytic and non-catalytic wall surfaces were considered.

Some of the early studies on the problem of extinction and ignition in forced convection systems has been reviewed by Fendell [3]. He has also considered the problem of flame ignition and extinction near the stagnation point region when an axisymmetric jet of oxidant flows from an upstream region at infinity against a reservoir of fuel. He applied inner and outer expansions to obtain the chemically frozen and equilibrium states. A plot of maximum temperature versus first Damköhler number was used to establish ignition and extinction characteristics. Two limits for the first Damköhler number were found. Below the lower limit there is no reaction. Beyond the upper limit the reactants are chemically in equilibrium. In between, the transition region is established.

Later, Tsuji and Yamaoka [17-19], Wu and Libby [20], Jones, Becker and Heinsohn [20] considered mainly the flame structure and properties without going into the ignition and extinction characteristics. Tsuji and Yamaoka [17-19] investigated the problem of counterflow diffusion flame in



the forward stagnation region of a porous cylinder. Various experiments were performed to analyze the flame structure with varying aerodynamic and chemical parameters. Wu and Libby [19] considered the behavior of the boundary layer at an axisymmetric stagnation region with hydrogen injection into a hot external airstream for the entire range from essentially frozen to essentially equilibrium flow. Jones, Becker and Heinsohn [21] studied the effect of an electric field on the concentration and temperature profiles of an opposed-jet diffusion flame. A computer simulation of a mathematical model of an opposed-jet methane/oxygen/nitrogen diffusion flame was presented which included a realistic set of chemical reactions and an electric field imposed on the flame.

The problem of opposed-jet diffusion flame was first treated by Spalding [11]. He developed an approximate procedure for evaluating the volumetric heat release rates and derived relations between the jet flow rate at extinction, the chemical kinetic constants and the laminar flame speed in premixed gases. Some of the conclusions of this analysis were later verified by the experimental work of Anagnostou and Potter [22].

In recent times, Chung, Fendell and Holt [23] considered the problem more systematically using boundary-layer approximations. A parameter consisting of various characteristics of the flame was developed by which "extinction"



state and "no-extinction" state could be distinguished. The problem was also formulated by Jain and Mukunda [12] for the case of an incompressible fluid with Prandtl and Schmidt numbers taken as unity. In particular, the problems of (i) a jet impinging on a wall of combustible material and (ii) the opposed-jet diffusion flame were studied. The effects of varying the wall temperature in case (i) and the jet temperature in case (ii) on the extinction speeds were considered. The effects of varying the activation energy and the free stream oxidant concentration in case (ii) were also investigated. Later Marathe and Jain [13] considered the problem of opposed-jet diffusion flame for several Lewis numbers. Solutions were obtained by using a modified flame surface theory, and extinction-ignition characteristics were resolved. The analysis showed that gases with high Lewis numbers are preferable for the purpose of flame stabilization.

The heat interaction between a premixed combustible mixture and a hot surface, at the stagnation region has been investigated to consider the effects of the hot surface on the ignition and extinction characteristics of the mixture. Some of the studies [4-7] were carried out using the Van't Hoff critical ignition condition, which states that a combustible mixture near the non-catalytic surface of a body will ignite when the temperature gradient normal to the wall is zero. Chambre [4] discussed the ignition phenomena in

a chemically reactive gas flowing about a heated body. Specifically the conditions at the forward stagnation point of the object were analyzed. A condition was formulated which relates the critical surface temperature for ignition with those parameters which control the heat and mass transport and the reaction kinetic mechanism. Sharma and Sirignano [5] investigated the ignition of a cold combustible mixture at the forward stagnation region of a hot projectile. The occurrence of a temperature maxima at the surface of the projectile acts as the ignition criterion. For quasi-stationary analysis, the characteristic parameter of the problem is the surface (or ignition) temperature. The steady boundary-layer equations describing the reacting flow have been solved numerically and the ignition temperatures for propane-air mixtures are calculated for different values of the various non-dimensional physical parameters. Alkidas and Durbetaki made a study on the ignition characteristics of a cold combustible mixture at the forward stagnation region of a flat plate [6]. Later they used a simplified model on three types of boundary layer flows: (i) planar stagnation flow, (ii) axisymmetric stagnation flow, and (iii) flow over a flat plate [7]. In both studies the Van't Hoff criterion was employed to find the ignition characteristics.

Alkidas and Durbetaki [8] have also carried out an analysis for the heat interaction between a combustible mixture and a constant-temperature wall near the stagnation

region of a blunt body without use of the Van't Hoff criterion. The steady-state governing equations have been solved numerically for a Lewis number equal to unity and for an incompressible fluid. The first Damköhler number was shown to critically influence the surface heat transfer.

All the studies discussed above were made with the assumption that the fluid was incompressible. Smith, Schmitz and Ladd [10] and Alkidas and Durbetaki [9] were the first to work the problem without the incompressibility assumption. Smith et al. [10] studied the theoretical steady-state and transient characteristics of a premixed combustible system in laminar axisymmetric stagnation flow by way of a numerical solution of the governing boundary-layer equations. Computations, which were based on the oxidation reaction of carbon monoxide in humid air, invoked a minimum of simplifying assumptions. Steady-state results included prediction of (1) profiles of the state variables, (2) extinction or blow off conditions, (3) ignition conditions and (4) the heat flux to the stagnation point. Alkidas and Durbetaki [9] examined the steady-state theories of ignition of a premixed gaseous mixture by a hot surface. Numerical results showed that the Van't Hoff criterion produces ignition temperature values that compare very favorably with values obtained by the absolute theory. At the same time, the values of the Ignition First Damköhler number calculated using the Van't Hoff criterion are in error by about 50 percent.



The study proposed here will be carried out for the interaction of a cold premixed combustible mixture with a hot inert gas in opposed flow. Two cases will be considered: (i) the hot inert gas is injected through a porous axisymmetric body, and (ii) both the hot inert gas and the premixed combustible mixture are free jets. The effects on the heat interaction and the ignition-extinction characteristics by varying the inert gas injection rate in case (i) and by varying the hot inert gas temperature in case (ii) are investigated. The first Damköhler number is an eigenvalue. The analysis is carried out for compressible flow and the Lewis number is taken as unity.

## CHAPTER III

### ANALYSIS

#### 3.1. Formulation of the Problem

##### 3.1.1. Statement of the Problem

The problem dealt with in this thesis is a stagnation flow of a premixed combustible mixture in opposed flow with a hot inert gas. The ignition characteristics of the combustible mixture by the hot inert gas are studied. Two cases of flow configuration are considered.

In the first case, a jet of fuel-oxidizer mixture is impinging on a blunt-nose body and the hot inert gas is injected through the porous wall. The wall is at constant temperature and is at the same temperature as the inert gas. The inert gas injection rate is varied to observe its effect on ignition characteristics. The detailed configuration is shown in Figure 1.

In the second case, a jet of fuel-oxidizer mixture is opposed by another jet of hot inert gas of equal momentum to form a stagnation region where the two jets meet. The inert gas temperature is varied to study its effect on the ignition characteristics. The velocity ratio of the two jets is adjusted to maintain the momentum constant for this case as can be seen in Figure 2.

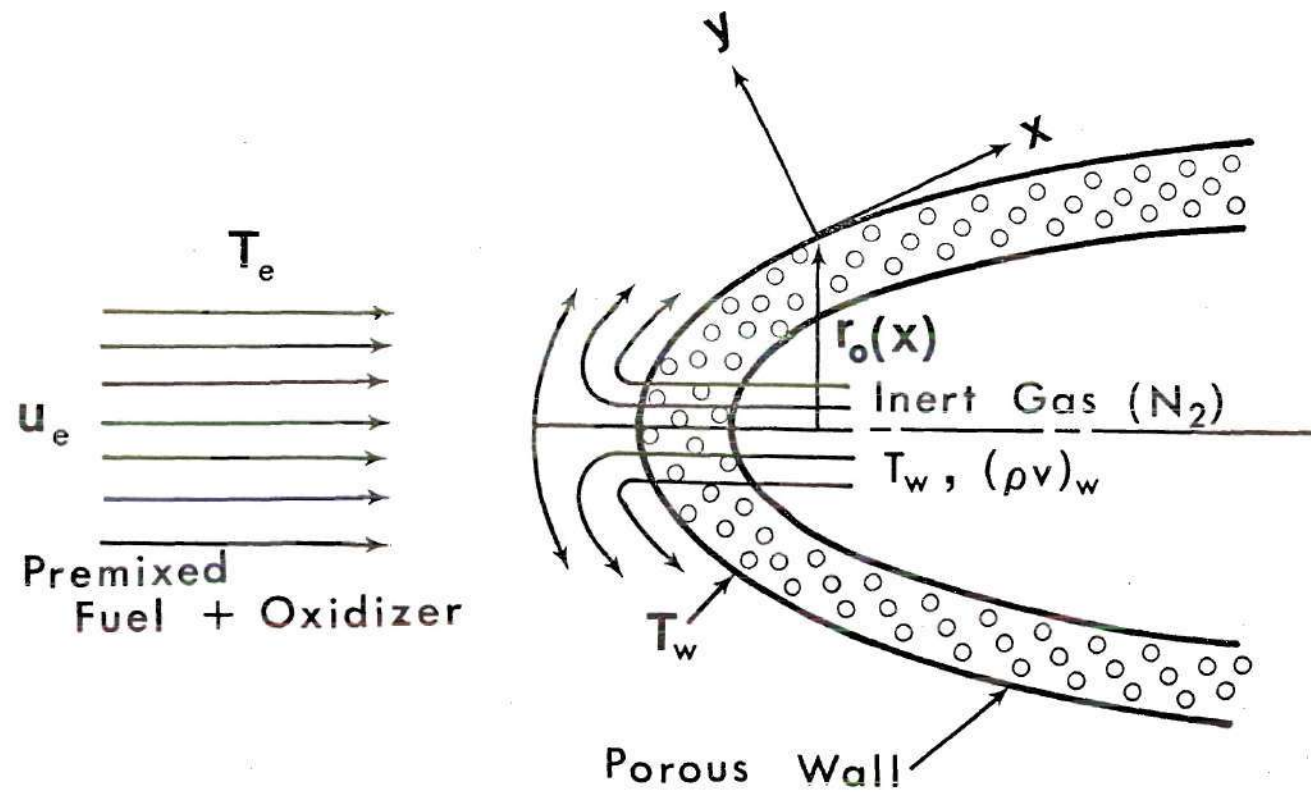


Figure 1. Coordinate System of an Impinging Jet

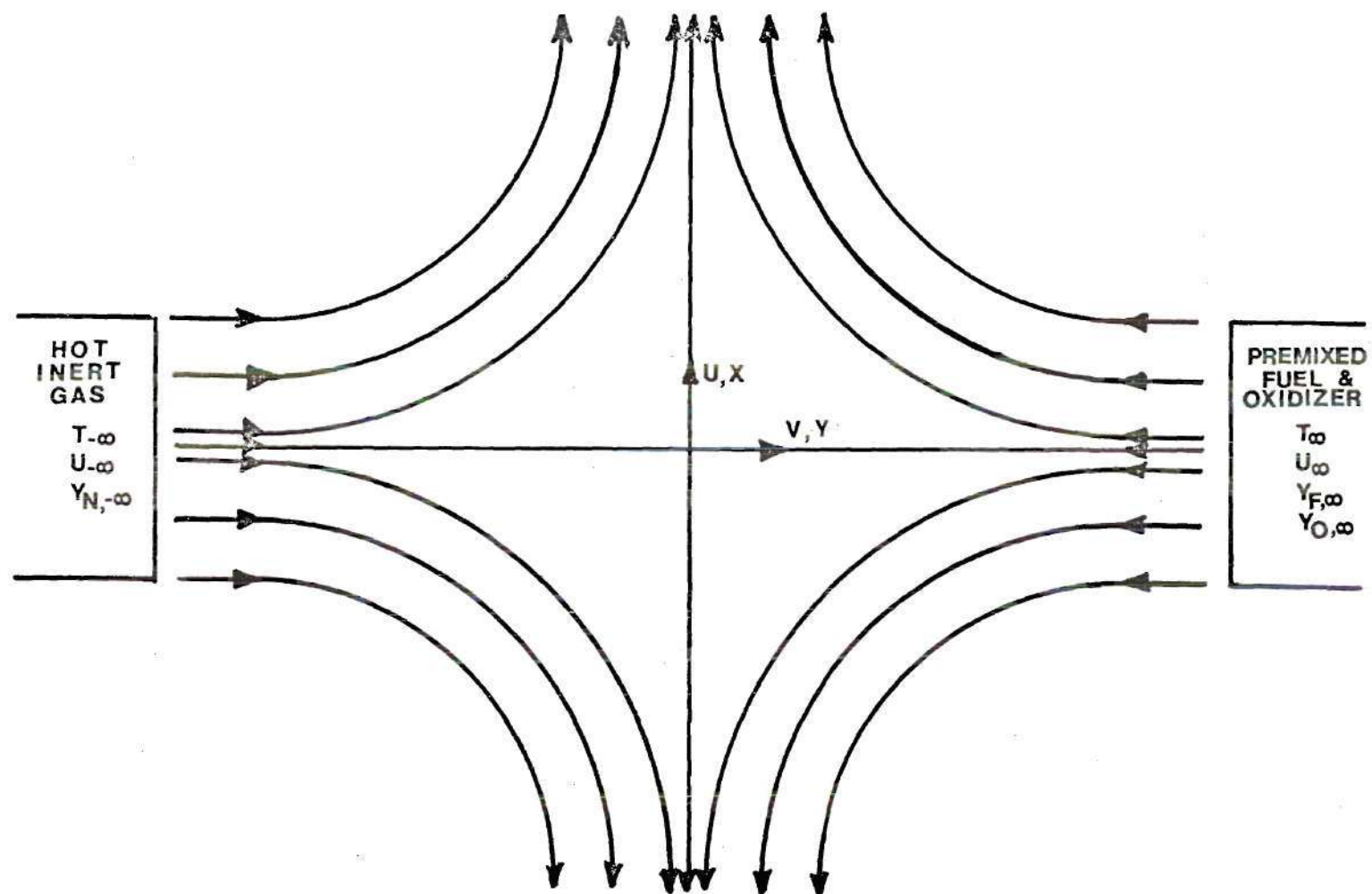


Figure 2. Coordinate System of Opposed-Jet

### 3.1.2. General Formulation

#### 3.1.2.1. Conservation Equations.

Continuity or Overall Mass Conservation

$$\partial \rho / \partial t + \nabla \cdot (\rho \vec{v}) = 0 \quad (3.1)$$

Momentum Conservation

$$\partial \vec{v} / \partial t + \vec{v} \cdot \nabla \vec{v} = - \nabla \cdot \bar{\bar{p}} / \rho + \sum_{i=1}^N Y_i \vec{f}_i \quad (3.2)$$

Energy Conservation

$$\rho (\partial U / \partial t) + \rho \vec{v} \cdot \nabla U = - \nabla \cdot \vec{q} - \bar{\bar{p}} : (\nabla \vec{v}) + \rho \sum_{i=1}^N Y_i \vec{f}_i \cdot \vec{v}_i \quad (3.3)$$

Species Conservation

$$\partial Y_i / \partial t + \vec{v} \cdot \nabla Y_i = \omega_i / \rho - [\nabla \cdot (\rho Y_i \vec{v}_i)] / \rho, \quad i = 1, 2, \dots, N \quad (3.4)$$

where

$\vec{f}_i$  = external force per unit mass on species  $i$

$N$  = total number of chemical species present

$\bar{\bar{p}}$  = pressure tensor

$\vec{q}$  = heat flux vector

$U$  = specific internal energy of the gas mixture



$\vec{V}_i$  = diffusion velocity of species i

$\vec{V}$  = mass-average velocity of species

$\omega_i$  = rate of production of species i by chemical reactions

$Y_i$  = mass fraction of species i

$\rho$  = density

### 3.1.2.2. Constitutive Equations.

Thermal equation of state

$$p = \rho RT \sum_{i=1}^N (Y_i/W_i) \quad (3.5)$$

Caloric equation of state

$$h_i = h_i^o + \int_{T_o}^T C_{p,i} dT, \quad i = 1, 2, \dots, N \quad (3.6)$$

Constitutive equation of momentum transport

$$\vec{\bar{p}} = [p + (\frac{2}{3} \mu - \ell) (\nabla \cdot \vec{V})] \vec{\bar{U}} - \mu [\nabla \vec{V} + (\nabla \vec{V})^T] \quad (3.7)$$

Constitutive equation of energy transport

$$\vec{q} = -k \nabla T + \rho \sum_{i=1}^N h_i Y_i \vec{V}_i + RT \sum_{i=1}^N \sum_{j=1}^N \left( \frac{X_j D_{T,i}}{W_i D_{ij}} \right) (\vec{V}_i - \vec{V}_j) \quad (3.8)$$

## Constitutive equation of chemical kinetics

$$\omega_i = W_i \sum_{k=1}^M (v_{i,k}'' - v_{i,k}') B_k T^{\alpha_k} e^{-(E_k/RT)} \quad (3.9)$$

where

$B_k$  = a constant in the frequency factor for the  $k^{\text{th}}$  reaction

$C_{p,i}$  = specific heat at constant pressure for species  $i$

$D_{ij}$  = binary diffusion coefficient for species  $i$  and  $j$

$D_{T,i}$  = thermal diffusion coefficient for species  $i$

$E_k$  = activation energy for the  $k^{\text{th}}$  reaction

$h_i$  = specific enthalpy of species  $i$

$h_i^0$  = standard heat of formation per unit mass for species  $i$  at temperature  $T_0$

$\ell$  = bulk viscosity coefficient

$M$  = total number of chemical reactions occurring

$p$  = hydrostatic pressure

$R$  = universal gas constant

$W_i$  = molecular weight of species  $i$

$X_i$  = mole fraction of species  $i$

$\alpha_k$  = exponent determining the temperature dependence of the frequency factor for the  $k^{\text{th}}$  reaction

$k$  = thermal conductivity

$\mu$  = coefficient of viscosity

$v_{i,k}'$  = stoichiometric coefficient for species  $i$  appearing as a reactant in reaction  $k$

$\nu_{i,k}''$  = stoichiometric coefficient for species  $i$   
appearing as a product in reaction  $k$

### 3.1.3. Boundary Layer Equation

To simplify the conservation equations and the constitutive equations, the following general assumptions are made

- (a) Laminar, steady-state flow.
- (b) Negligible body force.
- (c) Axisymmetric coordinates.
- (d) Low speed flow.
- (e) Boundary-layer approximation valid.

The most important assumption is (e) in which an order of magnitude analysis is made for the flow region inside the boundary layer, such that terms with orders of magnitude much smaller than other terms are neglected.

With the above assumptions the overall mass conservation equation (3.1) becomes

$$\frac{\partial}{\partial x} (\rho u x) + \frac{\partial}{\partial y} (\rho v x) = 0 \quad (3.10)$$

where  $u$  and  $v$  are velocity components in the tangential and normal direction to the surface respectively, and  $x$  and  $y$  are tangential and normal coordinates.

The momentum conservation equation (3.2) becomes

x-component

$$\rho u(\partial u/\partial x) + \rho v(\partial u/\partial y) = -(\partial p/\partial x) + \partial(\mu \frac{\partial u}{\partial y})/\partial y \quad (3.11)$$

y-component

$$\partial p/\partial y = 0 \quad (3.12)$$

To simplify the energy equation, some additional assumptions are made.

- (f) The specific heat coefficients of all species are the same and equal to a constant; i.e.,

$$C_{p,i} = C_{p,e} = C_p.$$

- (g) Four species exist in the flame: fuel, oxidizer, inert gas and products.

- (h) With thermal diffusion being neglected, the diffusion velocity is given by Fick's law,

$$\vec{V}_i = -D \nabla \ln Y_i \quad (3.13)$$

- (i) The binary diffusion coefficients of all species are the same; i.e.,  $D = D_i$ .

- (j) Radiation is negligible.

- (k) The heat flux is given by the expression

$$\vec{q} = -k \nabla T - \rho D \sum_i h_i \nabla Y_i \quad (3.14)$$

The energy conservation equation becomes

$$\rho u \frac{\partial T}{\partial x} + \rho v \frac{\partial T}{\partial y} = \frac{\partial}{\partial y} \left( k \frac{\partial T}{\partial y} \right) - \sum_i h_i^0 \omega_i, \quad i = F, O, N, P \quad (3.15)$$

Similarly the species conservation equation take the form

$$\rho u \frac{\partial Y_O}{\partial x} + \rho v \frac{\partial Y_O}{\partial y} = \frac{\partial}{\partial y} \left( \rho D \frac{\partial Y_O}{\partial y} \right) + \omega_O \quad (3.16)$$

$$\rho u \frac{\partial Y_F}{\partial x} + \rho v \frac{\partial Y_F}{\partial y} = \frac{\partial}{\partial y} \left( \rho D \frac{\partial Y_F}{\partial y} \right) + \omega_F \quad (3.17)$$

$$\rho u \frac{\partial Y_N}{\partial x} + \rho v \frac{\partial Y_N}{\partial y} = \frac{\partial}{\partial y} \left( \rho D \frac{\partial Y_N}{\partial y} \right) \quad (3.18)$$

Using the concept of overall chemical kinetics, it is assumed that the chemistry of the flame can be represented by



Since most of the reactions occurring in a flame are of second order, it is assumed that the reaction rate is governed by a second order Arrhenius kinetic expression, i.e.

$$\omega = B \rho^2 Y_O Y_F \exp(-E/RT) \quad (3.20)$$

where

$$\omega = - \frac{\omega_O}{v_O W_O} = - \frac{\omega_F}{v_F W_F} = \frac{\omega_P}{v_P W_P} \quad (3.21)$$

The product concentration can be determined by the following relationship

$$Y_O + Y_F + Y_N + Y_P = 1 \quad (3.22)$$

In equation (3.12), although  $\partial p / \partial y$  is of the order of unity, the variation of  $p$  in the normal direction is small. Therefore equation (3.11) becomes

$$\rho u \frac{\partial u}{\partial x} + \rho v \frac{\partial u}{\partial y} = - \frac{dp_e}{dx} + \frac{\partial}{\partial y} \left( \mu \frac{\partial u}{\partial y} \right) \quad (3.23)$$

where  $p_e$  is the pressure at the edge of the boundary-layer with the fact that  $p$  does not vary along a constant  $x$  line.

To determine the pressure gradient  $dp/dx$ , values at the edge of the boundary layer (or potential flow field) are substituted into equation (3.23). All the derivatives with respect to  $y$  vanish. Therefore, the relation is obtained.

$$\rho_e u_e \frac{du_e}{dx} = - \frac{dp}{dx} \quad (3.24)$$

The momentum equation is then



$$\rho u \frac{\partial u}{\partial x} + \rho v \frac{\partial u}{\partial y} = \rho_e u_e \frac{du_e}{dx} + \frac{\partial}{\partial y} \left( \mu \frac{\partial u}{\partial y} \right) \quad (3.25)$$

The heat flux in the normal direction can be expressed as

$$q = -k \frac{\partial T}{\partial y} - \rho D \sum_i h_i \left( \frac{\partial Y_i}{\partial y} \right) \quad (3.26)$$

#### 3.1.4. Boundary Conditions

3.1.4.1. The Impinging Jet. The boundary conditions for the impinging jet can be outlined in the following manner.

Momentum conservation

$$\text{at } y=0: \quad u=0 \quad (3.27a)$$

$$\text{at } y=0: \quad \rho v = (\rho v)_w = \text{constant} \quad (3.27b)$$

$$\text{as } y \rightarrow \infty: \quad u \rightarrow u_e = ax \quad (3.27c)$$

Equation (3.27b) indicates that the inert gas injection rate at the surface is constant. Equation (3.27c) assumes that the potential velocity in the neighborhood of the forward stagnation point is linearly proportional to the distance along the surface with the proportionality constant "a" defined as

$$a = U_{\infty}/d \quad (3.28)$$

where  $U_{\infty}$  is the jet velocity and  $d$  is the jet diameter.

Fuel conservation

$$\text{at } y = 0: \quad \rho v Y_F = \rho D \frac{\partial Y_F}{\partial y} \quad (3.29a)$$

$$\text{as } y \rightarrow \infty: \quad Y_F \rightarrow Y_{F,e} \quad (3.29b)$$

Oxidizer conservation

$$\text{at } y = 0: \quad \rho v Y_O = \rho D \frac{\partial Y_O}{\partial y} \quad (3.30a)$$

$$\text{as } y \rightarrow \infty: \quad Y_O \rightarrow Y_{O,e} \quad (3.30b)$$

Equations (3.29a) and (3.30a) indicate that no oxidizer or fuel cross the surface.

Inert gas conservation

$$\text{at } y = 0: \quad \rho v (Y_N - 1) = \rho D \frac{\partial Y_N}{\partial y} \quad (3.31a)$$

$$\text{as } y \rightarrow \infty: \quad Y_N \rightarrow Y_{N,e} \quad (3.31b)$$

Equation (3.31a) indicates that some inert gas is injected through the porous wall at a constant rate.



Energy conservation

$$\text{at } y = 0: \quad T = T_w \quad (3.32a)$$

$$\text{as } y \rightarrow \infty: \quad T \rightarrow T_e \quad (3.32b)$$

Equation (3.32a) imposes a constant wall temperature situation with the assumption that inert gas injected through the porous wall is at the same temperature.

3.1.4.2. The Opposed Jet. The boundary conditions for the opposed-jet are somewhat more complicated. They can be summarized in the following manner.

Momentum conservation

$$\text{at } y = 0: \quad v = 0 \quad (3.33a)$$

$$\text{as } y \rightarrow \infty: \quad u \rightarrow u_e = a_1 x \quad (3.33b)$$

$$\text{as } y \rightarrow -\infty: \quad u \rightarrow u_e = a_2 x \quad (3.33c)$$

The reference plane is taken to be the plane where no flow crosses. The proportionality constants for the potential velocities on both sides of the plane are  $a_1$  and  $a_2$ . In order for the flow not to cross the stagnation plane, a momentum balance must be achieved, i.e.

$$\rho_{\infty} U_{\infty}^2 = \rho_{-\infty} U_{-\infty}^2 \quad (3.34)$$

Assume the diameters of the jets are equal,

$$\rho_{\infty} a_1^2 = \rho_{-\infty} a_2^2 \quad (3.35)$$

With the help of the equation of state and by assuming constant average-molecular-weight, it is established that

$$\rho_{\infty} T_{\infty} = \rho_{-\infty} T_{-\infty} \quad (3.36)$$

or

$$a_2/a_1 = (T_{-\infty}/T_{\infty})^{1/2} \quad (3.37)$$

Fuel conservation

$$\text{as } y \rightarrow \infty: Y_F \rightarrow Y_{F,\infty} \quad (3.38a)$$

$$\text{as } y \rightarrow -\infty: Y_F \rightarrow 0 \quad (3.38b)$$

Oxidizer conservation

$$\text{as } y \rightarrow \infty: Y_O \rightarrow Y_{O,\infty} \quad (3.39a)$$

$$\text{as } y \rightarrow -\infty: Y_O \rightarrow 0 \quad (3.39b)$$

Inert gas conservation

$$\text{as } y \rightarrow \infty: Y_N = 0 \quad (3.40a)$$

$$\text{as } y \rightarrow -\infty: Y_N \rightarrow 1 \quad (3.40b)$$

Equations (3.38) and (3.39) indicate that oxidizer and fuel are on one side of the stagnation plane while equation (3.40) tells that inert gas is on the other side. It is a problem of fuel-oxidizer mixture mixing with a hot stream of inert gas from the opposite direction.

Energy conservation

$$\text{as } y \rightarrow \infty: T \rightarrow T_\infty \quad (3.41a)$$

$$\text{as } y \rightarrow -\infty: T \rightarrow T_{-\infty} \quad (3.41b)$$

The rate of  $T_{-\infty}/T_\infty$  is kept constant for each individual analysis. However, the ratio of  $a_2/a_1$  should also be kept constant so that the relationship in (3.37) is maintained.

### 3.2. Similarity Transformations

#### 3.2.1. Similarity Groups and Transformations

3.2.1.1. Purpose of the Transformation. The main purpose of the transformation is to transform the coordinate system into a new system such that the differential equations

become ordinary differential equations instead of partial differential equations. Therefore, the solution is given in terms of only the similarity variable  $\eta$  and independent of the other variable  $\xi$ .

3.2.1.2. General Techniques of Transformations. The well known Howarth-Dorodnitsyn transformation is used to obtain a self-similar set of equations. The coordinates  $\xi$  and  $\eta$  defined below are introduced.

$$\xi = \rho_e \mu_e a x^{2(m+1)/2(m+1)} \quad (3.42)$$

$$\eta = \left\{ \frac{\rho_e a(m+1)}{\mu_e} \right\}^{1/2} \int_0^y (\rho/\rho_e) dy \quad (3.43)$$

It may be noted that equations (3.34) and (3.35) have been obtained after introducing the potential solution near the stagnation point (i.e.  $u_e = ax$ ) into the general Howarth-Dorodnitsyn transformation. The values of "a" for various flow geometries are tabulated in Table 1, where  $m = 0$  for planar flow and  $m = 1$  for axisymmetric flow. Although every type of geometry mentioned in Table 1 can be studied with the present analysis, only the axisymmetric jet geometry is selected for this dissertation.

### 3.2.2. Transformation of the Governing Equations

Introducing the stream function  $\psi$  as defined by

Table 1. Values for Constant a

Geometry	Characteristic Dimension	a
Cylinder	R = radius of the cylinder	$2u_e/R$
Plane Jet (two dimensional)	h = width of the jet	$u_e/4h$
Axisymmetric Jet	D = diameter of the jet	$u_e/D$
Sphere	R = radius of the sphere	$3u_e/2R$

$$\rho u x^m = (\partial \psi / \partial y) \quad \text{and} \quad \rho v x^m = -(\partial \psi / \partial x) \quad (3.44)$$

and letting

$$\psi(\xi, \eta) = (2\xi)^{1/2} f(\eta) \quad (3.45)$$

the continuity equation is automatically satisfied. Further let

$$\alpha_i = Y_i / Y_{i,e} \quad (3.46)$$

and

$$\theta = T/T_e \quad (3.47)$$

and with the Howarth-Dorodnitsyn transformation, the momentum equation becomes

$$(Cf'')' + ff'' = \frac{1}{2} [(f')^2 - (\rho_e/\rho)] \quad (3.48)$$

where  $C = (\rho\mu)/(\rho\mu)_e$  is a constant. By using the equation of state equation (3.40) becomes

$$(Cf'')' + ff'' = \frac{1}{2} [(f')^2 - \theta] \quad (3.49)$$

Similarly the species conservation equations and the energy equation take the forms of

$$\left(\frac{C}{Sc} \alpha_F'\right)' + f\alpha_F' = \frac{1}{2} \nu_O W_O Y_{F,e} D_I \alpha_F \alpha_O \left(\frac{1}{\theta}\right) e^{-E^*/\theta} \quad (3.50)$$

$$\left(\frac{C}{Sc} \alpha_O'\right)' + f\alpha_O' = \frac{1}{2} \nu_F W_F Y_{O,e} D_I \alpha_F \alpha_O \left(\frac{1}{\theta}\right) e^{-E^*/\theta} \quad (3.51)$$

$$\left(\frac{C}{Sc} \alpha_N'\right)' + f\alpha_N' = 0 \quad (3.52)$$

and

$$\left(\frac{C}{Pr} \theta'\right)' + f\theta' = -\frac{1}{2} \nu_O W_O Y_{F,e}^2 D_I D_{II} \alpha_F \alpha_O e^{-E^*/\theta} \quad (3.53)$$

where  $D_I$  = first Damköhler number =  $B\rho_e/a$

$D_{II}$  = second Damköhler number  $q^0/C_{p,e} T_e \nu_F W_F$

$E^*$  = dimensionless activation energy =  $E/RT_e$

$Pr$  = Prandtl number =  $C_{p,e} \mu_e / k_e$



$$Sc = \text{Schmidt number} = \mu_e / \rho_e D$$

By combining equations (3.36) and (3.37)

$$u/u_e = f' \quad (3.54)$$

### 3.2.3. The Stoichiometry Measure

A measure of the stoichiometry of the reactants can be defined in the following manner,

$$n_e = \frac{Y_{O,e} v_F W_F}{Y_{F,e} v_O W_O} - 1 \quad (3.55)$$

For  $n_e = 0$  the mixture is in stoichiometric composition, while for  $n_e < 0$  the mixture is rich and for  $n_e > 0$  the mixture is lean.

With the aid of equation (3.14), the conservation of species equations (3.42) and (3.43) can be combined and readily integrated to give

$$\alpha_O = 1 - \frac{v_O W_O Y_{F,e}}{v_F W_F Y_{O,e}} (1 - \alpha_F) \quad (3.56)$$

or

$$\alpha_O = (\alpha_F + n_e) / (n_e + 1) \quad (3.57)$$

### 3.2.4. Boundary Conditions

3.2.4.1. The Impinging Jet Case. In the case for an impinging jet, the characteristic coefficient of the potential velocity  $a$  is taken to be  $u_e/d$  where  $u_e$  is the velocity at the edge of the boundary layer and  $d$  is the diameter of the jet. All the reference properties, temperature, and concentrations are evaluated at the free stream condition.

The transformed boundary conditions for an impinging jet with surface injection are as follows:

Momentum conservation

$$\text{at } \eta = 0: \quad f = f_w = -(\rho v)_w / (2\rho_e u_e a)^{1/2} \quad (3.58a)$$

$$\text{at } \eta = 0: \quad f' = 0 \quad (3.58b)$$

$$\text{as } \eta \rightarrow \infty: \quad f' \rightarrow 1 \quad (3.58c)$$

Fuel conservation

$$\text{at } \eta = 0: \quad \frac{C}{Sc} \alpha_F' = -f_w \alpha_F \quad (3.59a)$$

$$\text{as } \eta \rightarrow \infty: \quad \alpha_F \rightarrow 1 \quad (3.59b)$$

Oxidizer conservation

$$\text{at } \eta = 0: \quad \frac{C}{Sc} \alpha_0' = -f_w \alpha_0 \quad (3.60a)$$

$$\text{as } \eta \rightarrow \infty: \quad \alpha_0 \rightarrow 1 \quad (3.60b)$$

Inert gas conservation

$$\text{at } \eta = 0: \quad \frac{C}{Sc} \alpha_N' = -f_w (\alpha_N - \frac{1}{Y_{N,e}}) \quad (3.61a)$$

$$\text{as } \eta \rightarrow \infty: \quad \alpha_N \rightarrow 1 \quad (3.61b)$$

Energy conservation

$$\text{at } \eta = 0: \quad \theta = \theta_w \quad (3.62a)$$

$$\text{as } \eta \rightarrow \infty: \quad \theta \rightarrow 1 \quad (3.62b)$$

3.2.4.2. The Opposed-Jet Case. For an opposed-jet flow there are two coefficients of the potential velocity,  $a_1$  and  $a_2$ , one on each side of the stagnation plane. These are defined as follows

$$a_1 = U_\infty/d \quad \text{and} \quad a_2 = U_{-\infty}/d$$

where  $U_\infty$  and  $U_{-\infty}$  are the jet velocities of the combustible mixture jet and inert gas jet respectively, and  $d$  is the

diameter of both jets. The coefficient  $a_1$  is arbitrarily taken to be the characteristic value and is used in the similarity transformation. All the reference properties, temperature, and concentrations of all species except the inert gas are evaluated at infinity, i.e. free stream at the fuel-oxidizer side. Concentration of the inert gas is referenced by  $Y_{N,-\infty}$ , which is then unity for the present problem.

The transformed boundary conditions for the opposed-jet case are as follows:

Momentum conservation

$$\text{at } \eta = 0: f = 0 \quad (3.63a)$$

$$\text{as } \eta \rightarrow \infty: f' \rightarrow 1 \quad (3.63b)$$

$$\text{as } \eta \rightarrow -\infty: f' \rightarrow (\theta_{-\infty})^{1/2} \quad (3.63c)$$

Fuel conservation

$$\text{as } \eta \rightarrow \infty: \alpha_F \rightarrow 1 \quad (3.64a)$$

$$\text{as } \eta \rightarrow -\infty: \alpha_F \rightarrow 0 \quad (3.64b)$$

Oxidizer conservation

$$\text{as } \eta \rightarrow \infty: \alpha_O \rightarrow 1 \quad (3.65a)$$

$$\text{as } \eta \rightarrow -\infty: \alpha_O \rightarrow 0 \quad (3.65b)$$

Inert gas conservation

$$\text{as } \eta \rightarrow \infty: \alpha_N \rightarrow 0 \quad (3.66a)$$

$$\text{as } \eta \rightarrow -\infty: \alpha_N \rightarrow 1 \quad (3.66b)$$

Energy conservation

$$\text{as } \eta \rightarrow \infty: \theta \rightarrow 1 \quad (3.67a)$$

$$\text{as } \eta \rightarrow -\infty: \theta \rightarrow \theta_{-\infty} \quad (3.67b)$$

The boundary condition (3.63c) is so imposed as to satisfy the momentum balance in equation (3.37). It should also be noted that the pressure gradient term in equation (3.11) will be expressed in different ways on each side of the stagnation plane. However, they have the same value. This statement can be verified considering the following expression

$$\rho_{\infty} u_{\infty} \frac{du_{\infty}}{dx} = \rho_{\infty} (a_1 x) (a_1) = \rho_{\infty} a_1^2 x \quad (3.68)$$

$$\rho_{-\infty} u_{-\infty} \frac{du_{-\infty}}{dx} = \rho_{-\infty} (a_2 x) (a_2) = \rho_{-\infty} a_2^2 x \quad (3.69)$$



and since

$$\frac{a_2}{a_1} = (\theta_{-\infty})^{1/2} = (\rho_{\infty}/\rho_{-\infty})^{1/2} \quad (3.70)$$

then

$$\rho_{-\infty} u_{-\infty} \frac{du_{-\infty}}{dx} = \rho_{\infty} u_{\infty} \frac{du_{\infty}}{dx} \quad (3.71)$$

Consequently the pressure gradients are the same on both sides of the stagnation plane.

## CHAPTER IV

## METHOD OF SOLUTION

4.1. Further Simplification of the  
Governing Equations

A further simplification can be made on the normalized system of differential equations by considering the following additional assumptions:

(j) Lewis number is equal to unity,  $Sc = Pr$ .

(k)  $C = 1$ , i.e.  $\rho\mu = \rho_e\mu_e = \text{constant}$ .

Assumptions (j) and (k) are usual practice in combustion theory. With the relations in equations (3.49)-(3.53) and the dimensionless groups

$$\bar{D}_I = \frac{1}{2} \nu_O W_O Y_{F,e} D_I \quad (4.1)$$

and

$$\bar{D}_{II} = Y_{F,e} D_{II} \quad (4.2)$$

the equations can be rewritten as

$$f''' + f'' = \frac{1}{2} [(f')^2 - \theta] \quad (4.3)$$

$$\alpha_F'' + Sc f \alpha_F' = \bar{D}_I Sc (n_e + \alpha_F) \alpha_F (1/\theta) e^{-E^*/\theta} \quad (4.4)$$

$$\alpha_N'' + Sc f \alpha_N' = 0 \quad (4.5)$$

and

$$\theta'' + Pr f \theta' = -Pr \bar{D}_I \bar{D}_{II} (n_e + \alpha_F) \alpha_F (1/\theta) e^{-E^*/\theta} \quad (4.6)$$

The above equations can then be solved numerically with the boundary conditions (3.58) to (3.67).

#### 4.2. Method

In order to solve the system of differential equations numerically, the unknown initial conditions have to be estimated and adjusted to meet the known asymptotic conditions.

The Adams-Moulton integration subroutine [24] is used to integrate the three simultaneous equations, (4.3), (4.4) and (4.6), with the assumed initial conditions. The asymptotic solution is then compared with the known asymptotic conditions. The initial conditions are adjusted with the deviations by using the Newton-Raphson Iteration Method until a satisfactory solution is obtained.

### 4.3. The Impinging Jet Solution

#### 4.3.1. The Boundary Conditions

The boundary conditions can be divided into two groups: the initial conditions and the asymptotic conditions. The initial conditions for this case are

$$\text{at } \eta = 0: \quad f = f_w, \quad f' = 0$$

$$\alpha_F' = -Sc \, f \alpha_F$$

$$\theta = \theta_w$$

while the asymptotic conditions are

$$\text{as } \eta \rightarrow \infty: \quad f' \rightarrow 1$$

$$\alpha_F \rightarrow 1$$

$$\theta \rightarrow 1$$

The total order of the three equations is seven. Therefore, the number of boundary conditions is also seven.

#### 4.3.2. Procedure of Solution

(i) The quantities  $f''(0) = \zeta_1$ ,  $\alpha_F(0) = \zeta_2$ , and  $\theta'(0) = \zeta_3$  are initially assumed.

(ii) The Adams-Moulton integration subroutine is used to integrate the three simultaneous equations, (4.3), (4.4) and (4.6), with the above assumed initial conditions in addition to the known initial conditions. Taken into

consideration are also the derivatives of each dependent variable with respect to each  $\zeta$ .

(iii) The computed values of  $f'(\infty)$ ,  $\alpha_F(\infty)$ , and  $\theta(\infty)$  are compared with the known asymptotic boundary conditions,  $f' \rightarrow 1$ ,  $\alpha_F \rightarrow 1$  and  $\theta \rightarrow 1$ . Infinity ( $\infty$ ) is treated as a large value of  $\eta$  such that the solution becomes asymptotic at that location.

(iv) The above deviations are computed and put into the Newton-Raphson Iteration Method to predict the adjustment that should be made on the  $\zeta$ 's.

(v) Steps (ii) through (iv) are repeated several times until the error as defined by the following equation is less than  $10^{-8}$

$$\begin{aligned} \text{Error} = & [f'(\infty) - 1]^2 + [\alpha_F(\infty) - 1]^2 + [\theta(\infty) - 1]^2 + \\ & [f''(\infty)]^2 + [\alpha_F'(\infty)]^2 + [\theta(\infty)]^2 \end{aligned} \quad (4.7)$$

#### 4.4. The Opposed-Jet Solution

##### 4.4.1. The Boundary Conditions

The boundary conditions in this case can be divided into three groups: the initial conditions, the positive asymptotic conditions and the negative asymptotic conditions. The initial condition known in this case is



$$\text{at } \eta = 0: \quad f = 0$$

The positive asymptotic conditions are

$$\text{as } \eta \rightarrow \infty: \quad f' \rightarrow 1$$

$$\alpha_F \rightarrow 1$$

$$\theta \rightarrow 1$$

while the negative asymptotic conditions are

$$\text{as } \eta \rightarrow -\infty: \quad f' \rightarrow \theta_{-\infty}^{1/2}$$

$$\alpha_F \rightarrow 0$$

$$\theta \rightarrow \theta_{-\infty}$$

#### 4.4.2. Procedure of Solution

The procedure in the opposed-jet case is more or less similar to the one in the impinging jet case. However, in this case six initial conditions have to be assumed. The integration has to be performed in two directions and the error is defined as

$$\begin{aligned} \text{Error} = & [f'(\infty) - 1]^2 + [\alpha_F(\infty) - 1]^2 + [\theta(\infty) - 1]^2 + [f''(\infty)]^2 \\ & + [\alpha_F'(\infty)]^2 + [\theta'(\infty)]^2 + [f'(-\infty) - \theta_{-\infty}^{1/2}]^2 + [\alpha_F(-\infty) - 0]^2 \\ & + [\theta(-\infty) - \theta_{-\infty}]^2 + [f''(-\infty)]^2 + [\alpha_F'(-\infty)]^2 + [\theta'(-\infty)]^2 \quad (4.8) \end{aligned}$$

#### 4.5. Specification of Parameters

The numerical computation is carried out using the following values of dimensionless parameters and boundary conditions for the governing equations:

$$\text{Pr} = 0.74, \text{Sc} = 0.74, E^* = 67.1366,$$

$$\bar{D}_{II} = 6.44518, n_e = 0, \theta_w \text{ or } \theta_{-\infty} = 3.0$$

These values correspond to the case of an incoming stoichiometric mixture of methane and oxygen at a temperature of 300°K and an activation energy of 40 kcal/g-mole. Additionally the impinging jet problem is worked out with different injection rates of inert gas at  $f_w = -0.05, -0.25, -0.30, -0.50$ .

#### 4.6. Numerical Method

##### 4.6.1. Introduction

The numerical solution of the ordinary differential equations of boundary-layer theory involves the satisfaction of asymptotic boundary conditions; that is, some boundary conditions are specified at the initial point and others are specified as limits that must be approached at large values of the independent variable, corresponding to the edge of the boundary layer. In order to integrate the differential equations numerically from the initial point to the edge of

the boundary layer, it is necessary to specify as many additional conditions at the initial point as there are conditions to be satisfied at the edge of the boundary layer. All methods that have been used to find the proper initial conditions rely on the fact that, for large values of the independent variable, the integrals of the differential equations depend on the initial conditions. One method that has been used to find the proper initial conditions, called the initial-value method [25], is that of obtaining integrals of the differential equations with assumed initial conditions, that is, an attempt is made to integrate the differential equations to the edge of the boundary layer. If this can be accomplished, corrections are made for the initial assumed values by the Newton-Raphson Method, and the process is repeated until convergence is achieved.

Another method that has been used, called quasi-linearization [26], is similar in principle to the initial-value method except that the original differential equations are linearized. The resulting linear differential equations for the current approximation are inhomogeneous, since they also contain the previous approximation as members. A disadvantage associated with the quasilinearization method is that functions representing the previous approximation have to be stored in order to construct the current approximation. Furthermore, the solution of the inhomogeneous equation obtained by combining complementary solutions and a

particular integral is usually not well determined except near the origin or initial points, as pointed out by Hartree [27].

Neither of these methods, however, has solved the problem of when to stop the integration. In the various methods, the value of the independent variable defined at the boundary layer edge must be estimated beforehand. If the estimated value is too small, the integrals of the differential equations may not be able to satisfy the imposed conditions; or, there may be more than one value of an initial condition that leads to integrals that satisfy the imposed boundary conditions. If the estimated value is too large, it is possible that the integral will diverge or that convergence to a solution is extremely slow.

Another problem that sometimes besets the numerical integration of the boundary-layer equations is the apparent insensitivity of the integrals to the initial conditions. This difficulty appears in the integration of the Falkner-Skan equation [28]. In an effort to adapt the initial-value method to the solution of differential equations with asymptotic boundary conditions, a method was developed for the present study to eliminate the problem of when to stop integration. This method is capable of satisfying the boundary conditions at the edge of the boundary layer correctly; that is the boundary values are approached asymptotically. This is accomplished by choosing the



additional initial conditions so that the mean square error between the computed variable and the asymptotic values is minimized. A method of solution was developed which is based on the least-square convergence criterion in which the edge of the boundary layer is approached in steps. The convergence rate to a solution is rapid, and convergence appears to be insensitive to the initial guesses of the initial conditions. Use of a least square convergence criterion leads to a unique solution. It is this method that was used to obtain the results presented in Chapter V.

#### 4.6.2. Discussion of the Method

Three things have to be considered with caution when this method is applied to the solution of the problem of ignition and extinction characteristics.

(i) A proper limit of integration for the first approximation has to be chosen carefully. When a large  $\eta_{\text{end}}$  is used, the solution might diverge before the integration is performed to  $\eta_{\text{end}}$ . When a small  $\eta_{\text{end}}$  is used, the solution is far from its asymptotic solution and the error is bound to be large.

(ii) For the multivalued solution, one of the solutions is more stable than the others. Therefore, when a small  $\eta_{\text{end}}$  is used for iteration, the solution will always converge to the most stable one no matter what initial values are assumed. Consequently a larger  $\eta_{\text{end}}$  should be used when an unstable solution is sought.



(iii) In certain ranges of  $\bar{D}_I$ , there are two solutions near the upper branch of  $\theta_{\max}$  versus  $\bar{D}_I$ . One of the solutions yields a negative fuel concentration profile which is physically unrealistic, although mathematically valid. Since the two solutions are close and the unrealistic solution is more stable, it is difficult to obtain the other solution. A method is applied to guarantee in the temperature profile a maximum temperature  $\theta_{\max}$  which does not occur in the unrealistic solution. Instead of using the stagnation plane ( $f = 0$ ) as  $\eta = 0$  plane, the plane  $\theta' = 0$  where maximum temperature occurs is used as the starting point of the independent variable  $\eta$ . The initial estimate for the fuel concentration at  $\eta = 0$  and  $\theta' = 0$ , where normally a negative value is yielded, is purposely chosen to be a positive value. A satisfactory solution can then be achieved.

The numerical scheme is very efficient for a complicated problem like this although a few modifications had to be made. It is recommended that the method be used to solve boundary-layer type problems.

## CHAPTER V

### RESULTS AND DISCUSSION

The numerical results presented in this thesis are calculated following the procedures outlined in Chapter IV.

Emphasis is placed on establishing the flow transition from "frozen" flow to chemical equilibrium flow and the associated ignition criteria. The study is also concerned with the variation of pertinent parameters such as velocity, temperature, and mass fraction within the boundary layer.

Generally speaking, two major types of results are presented. The first group of results consists of profiles of velocity, mass fraction, and temperature. These results, especially in graphical forms, describe the variation of temperature, velocity, and mass fraction with respect to the similarity variable (the dimensionless position coordinate) with the first Damköhler number as a parameter. The second type of results illustrates the transition from equilibrium flow to frozen flow. The results are presented for each solution in the form of characteristic values such as the fuel mass fraction at the wall  $\alpha_{F,w}$ , the heat transfer rate at the wall  $Nu/Re^{1/2}$ , the skin friction coefficient at the wall  $f_w''$ , the maximum temperature  $\theta_{max}$  versus the first Damköhler number  $\bar{D}_I$ . The transition region as mentioned in

the previous chapters is multivalued. Therefore, a maximum first Damköhler number is defined as the critical first Damköhler number for ignition. The critical first Damköhler number then represents a lower limit beyond which ignition of the combustible mixture takes place. The ignition characteristics of the combustible mixture are studied through these cases.

Additional results, such as the effect of inert gas injection rate on ignition point  $\bar{D}_{I,i}$  in the impinging jet case as well as on heat transfer rate at the interface  $Nu/Re^{1/2}$ , with  $\bar{D}_I$  as a parameter are also studied.

## 5.1. Results of the Impinging Jet

### 5.1.1. Fuel Mass Fraction at the Wall

The dependence of the fuel mass fraction at the wall on the first Damköhler number is shown in Figure 3. It is divided into two regions. In branch A, where frozen flow phenomenon is more significant,  $\alpha_{F,w}$  decreases with increasing  $\bar{D}_I$ . In branch B, where equilibrium flow phenomenon is more dominating,  $\alpha_{F,w}$  increases with increasing  $\bar{D}_I$ . The two branches meet at the characteristic first Damköhler number,  $\bar{D}_{I,i}$ , where ignition occurs. Beyond  $\bar{D}_{I,i}$  equilibrium is reached and ignition takes place. The trace of variation of  $\alpha_{F,w}$  from frozen to equilibrium flow is called a characteristic curve of ignition at a certain injection rate. For each injection rate, there is a unique characteristic curve

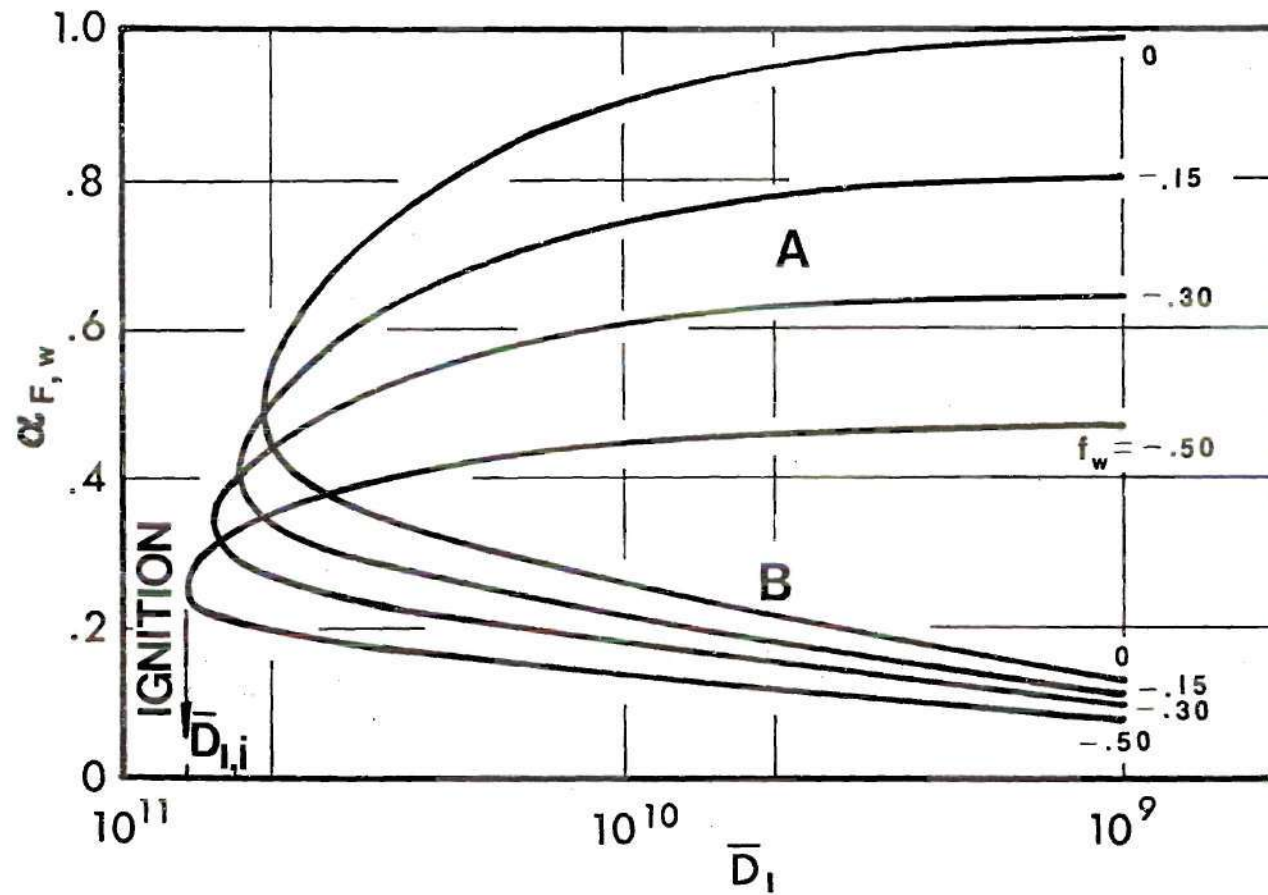


Figure 3. The Fuel Concentration at the Interface as a Function of the First Damköhler Number with Inert Gas Injection Rate as a Parameter,  $\theta_w = 3.0$



with its own  $\bar{D}_{I,i}$ . In the no injection case, the fuel mass fraction at the wall reaches a maximum value of unity and the fuel mass fraction at the wall decreases as injection rate is increased.

#### 5.1.2. Dependence of Skin Friction on $\bar{D}_I$

The dependence of skin friction on the first Damköhler number is shown in Figure 4. It decreases as the flow goes through the transition from "equilibrium" to "frozen." A maximum value of  $\bar{D}_I$  is reached at the characteristic first Damköhler number  $\bar{D}_{I,i}$ . The general trend shows that higher injection rates lower skin friction. This can be attributed to the fact that higher injection rates push the peak temperature and also the maximum velocity further away from the surface and reduce the velocity gradient near the wall.

#### 5.1.3. Heat Transfer Rate Dependence on $\bar{D}_I$

The dependence of heat transfer rate  $Nu/Re^{1/2}$  on the first Damköhler number  $\bar{D}_I$  is illustrated in Figure 5. The heat transfer to the wall decreases during the flow transition from "equilibrium" to "frozen." The direction of the heat transfer is toward the surface from a reaction zone near the surface. Therefore,  $Nu/Re^{1/2}$  is positive in branch B. While in branch A, the heat transfer is from the surface to the free stream since there is not much reaction occurring. For this region  $Nu/Re^{1/2}$  is negative.

The heat transfer rate is higher at the lower injection rates in branch B. This is due to the dilution of the



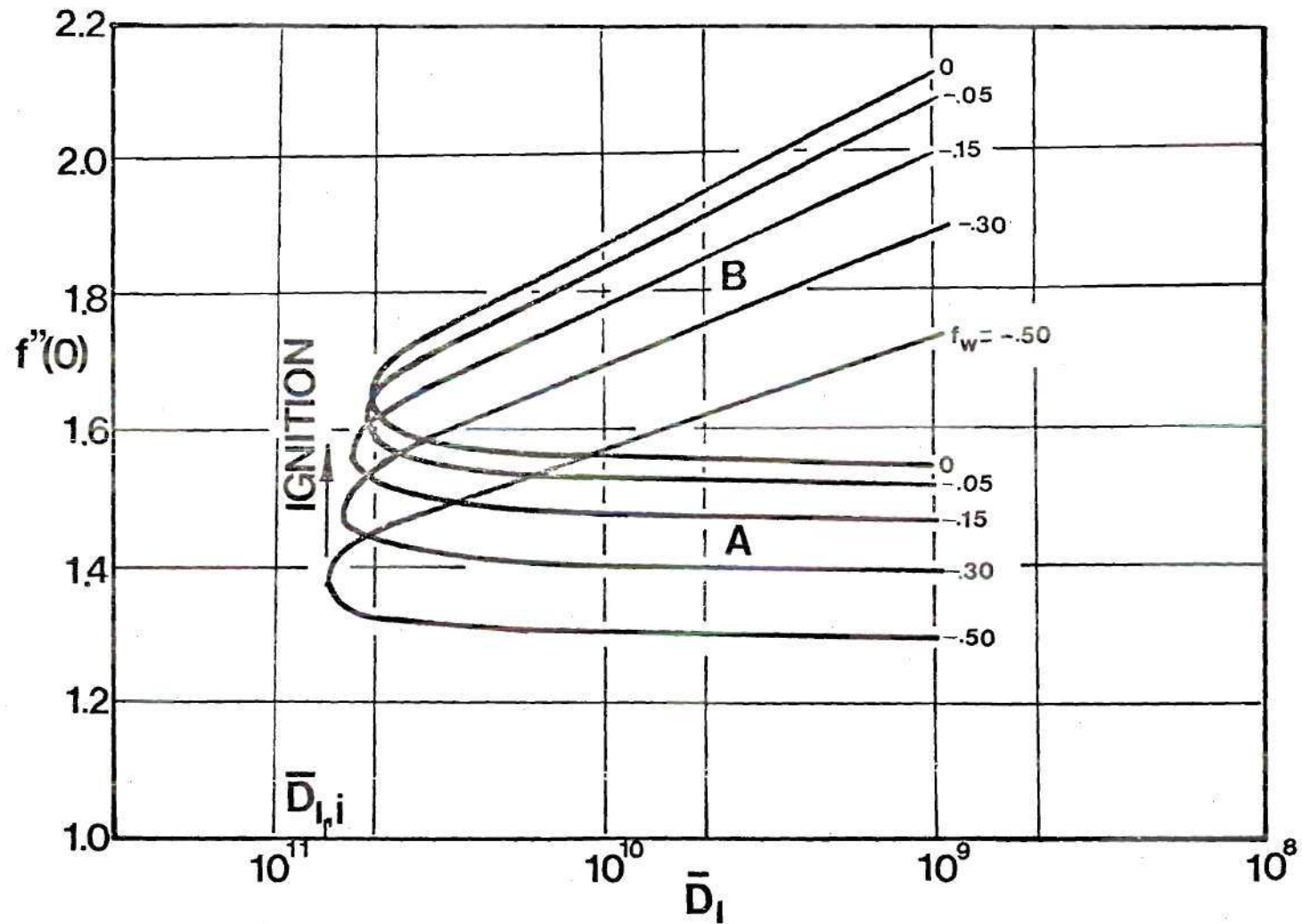


Figure 4. Dependence of the Skin Friction on the First Damköhler Number with Inert Gas Injection Rate as a Parameter,  $\theta_w = 3.0$

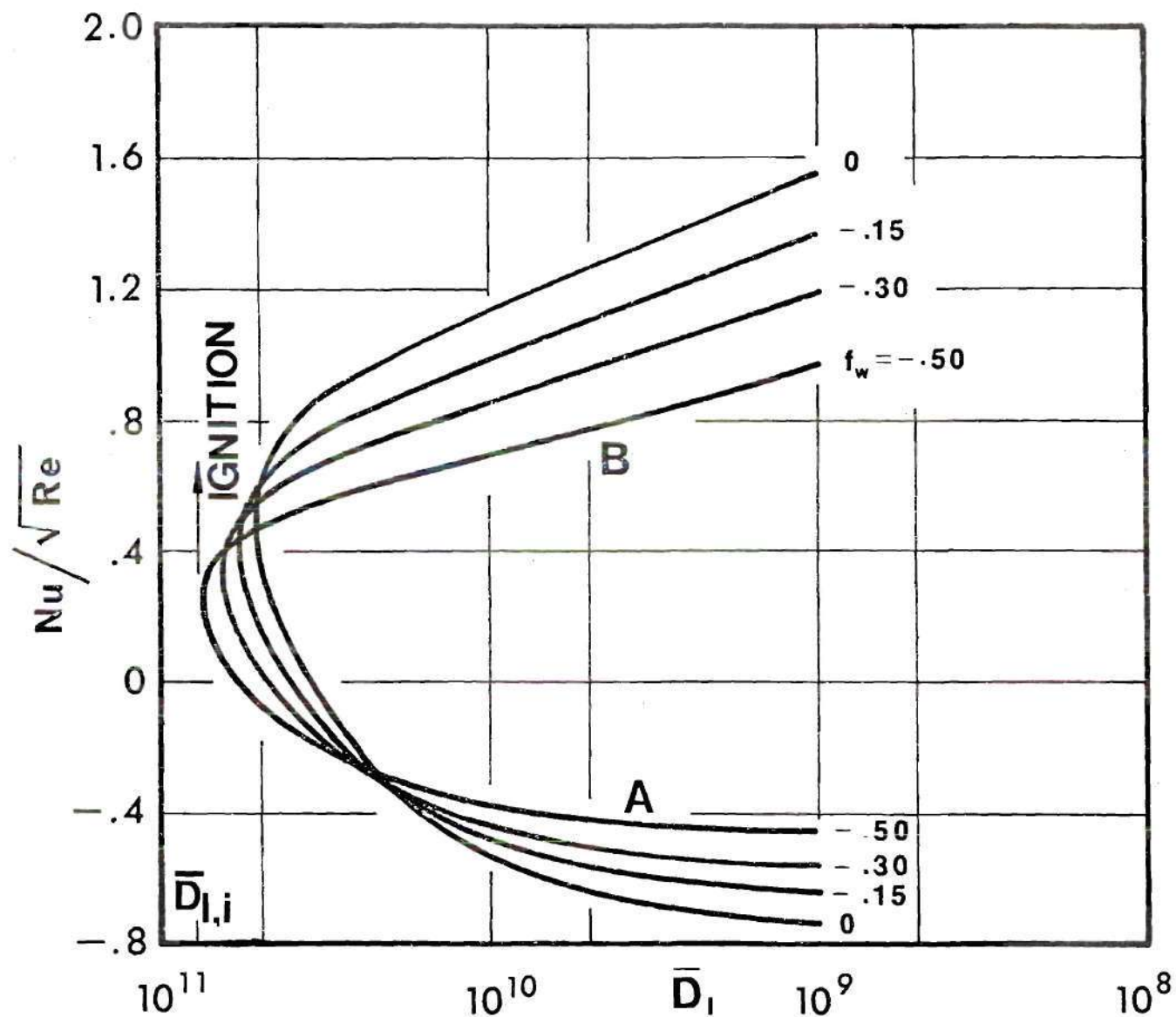


Figure 5. Dependence of Surface Heat Transfer Rate on the First Damköhler Number with Inert Gas Injection Rate as a Parameter,  $\theta_w = 3.0$

mixture by the inert gas injection and the displacement of the reaction zone further away from the wall due to injection. Therefore, the heat transfer rate is slower. In branch A, the heat transfer is in the opposite direction. The temperature gradient at wall decreases with inert gas injection. Therefore, the heat transfer rate from the surface to the free stream is slower with the higher injection rate.

#### 5.1.4. Velocity Distribution

A comparison of the velocity profiles at different stages of the flow transition in the impinging jet case is shown in Figure 6. The normalized temperature of the hot inert gas at the wall is held constant at  $\theta = 3$ . The injection rate  $f_w$ , and the first Damköhler number  $\bar{D}_I$  are flow parameters. It is shown that for constant  $\bar{D}_I$ , maximum velocity is higher for higher injection rate of inert gas. This is due to the fact that the inert gas increases the temperature of the combustible mixture and decreases the density. This eventually creates a higher velocity. The higher rate of injection carries the hot inert gas away from the surface to have a peak velocity further away from the surface.

Under constant injection rate, flows in the near-equilibrium branch, branch B, achieve a higher maximum velocity than in branch A, the near-frozen branch. It is clear that flows with faster chemical reaction rate will achieve a higher temperature as more heat is generated.

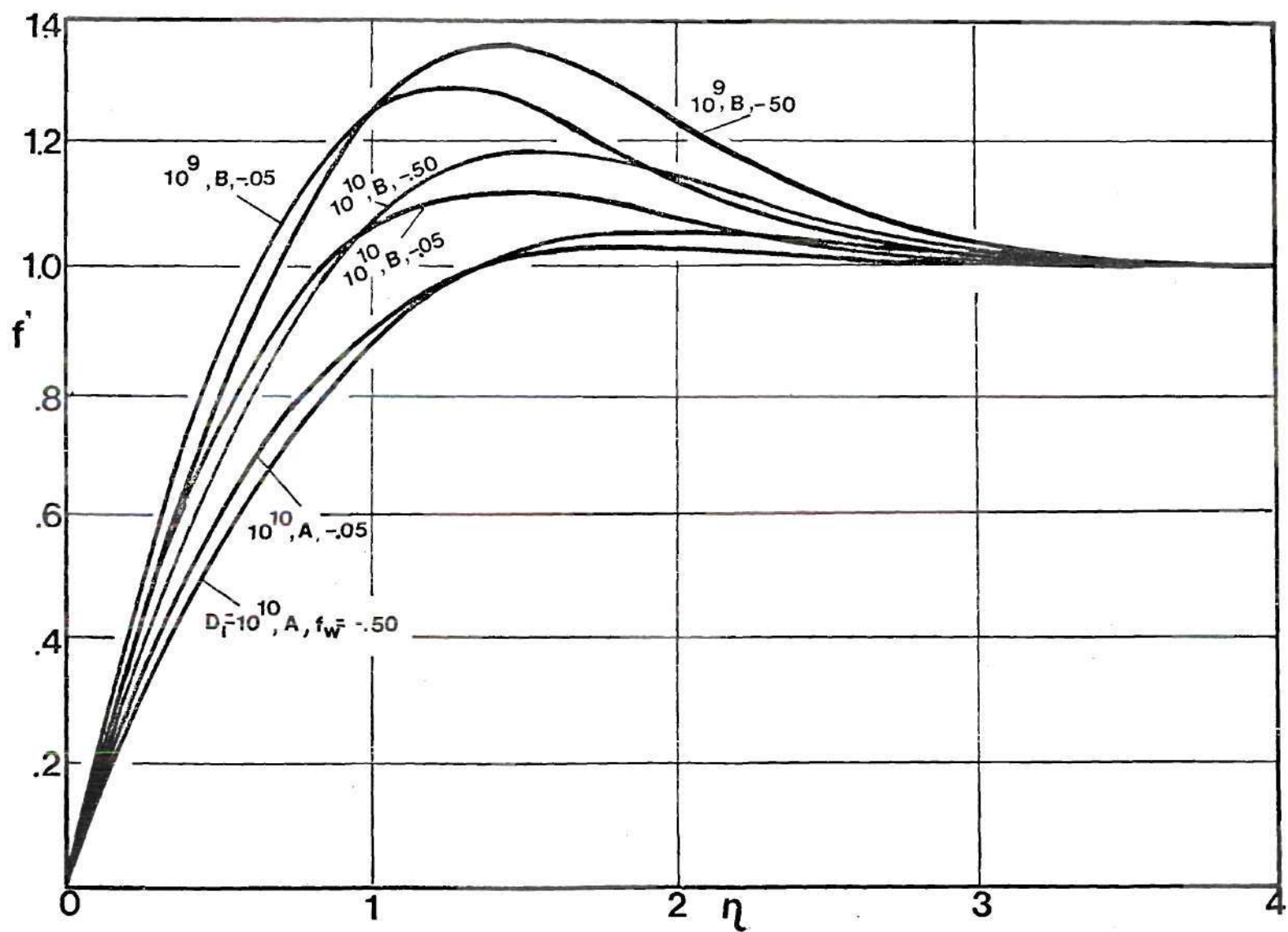


Figure 6. Comparison of Velocity Profiles at Specified Damköhler Number and Inert Gas Injection Rates



Consequently the density decreases and flow velocity increases. It should be noticed that the velocity profiles in branch B peak over the free stream velocity within the boundary layer. This is due to a sudden decrease in density. This feature can only be investigated through the compressible consideration. With incompressible assumption, the velocity can never be greater than the free stream velocity.

#### 5.1.5. Fuel Concentration Profiles

A comparison of the fuel concentration profiles in the boundary layer is shown in Figure 7. The normalized temperature is held constant at  $\theta_w = 3$ , with  $f_w$  and  $\bar{D}_I$  as parameters.

The fuel concentration near the wall is lower for the higher injection rate due to the dilution of the mixture by the inert gas injection. The fuel concentration also decrease as the flow transition goes from "frozen" to "equilibrium" flow. Apparently, the chemical reaction reduces the fuel composition while it produces more products. At frozen flow and no inert gas injection the dimensionless fuel mass fraction  $\alpha_F$  is constant and equal to unity throughout the boundary layer. This is the upper bound for all the fuel concentration profiles. The lower bound is when the flow is at equilibrium and the injection rate is very high. Then there will be total consumption of the fuel before it reaches the wall.



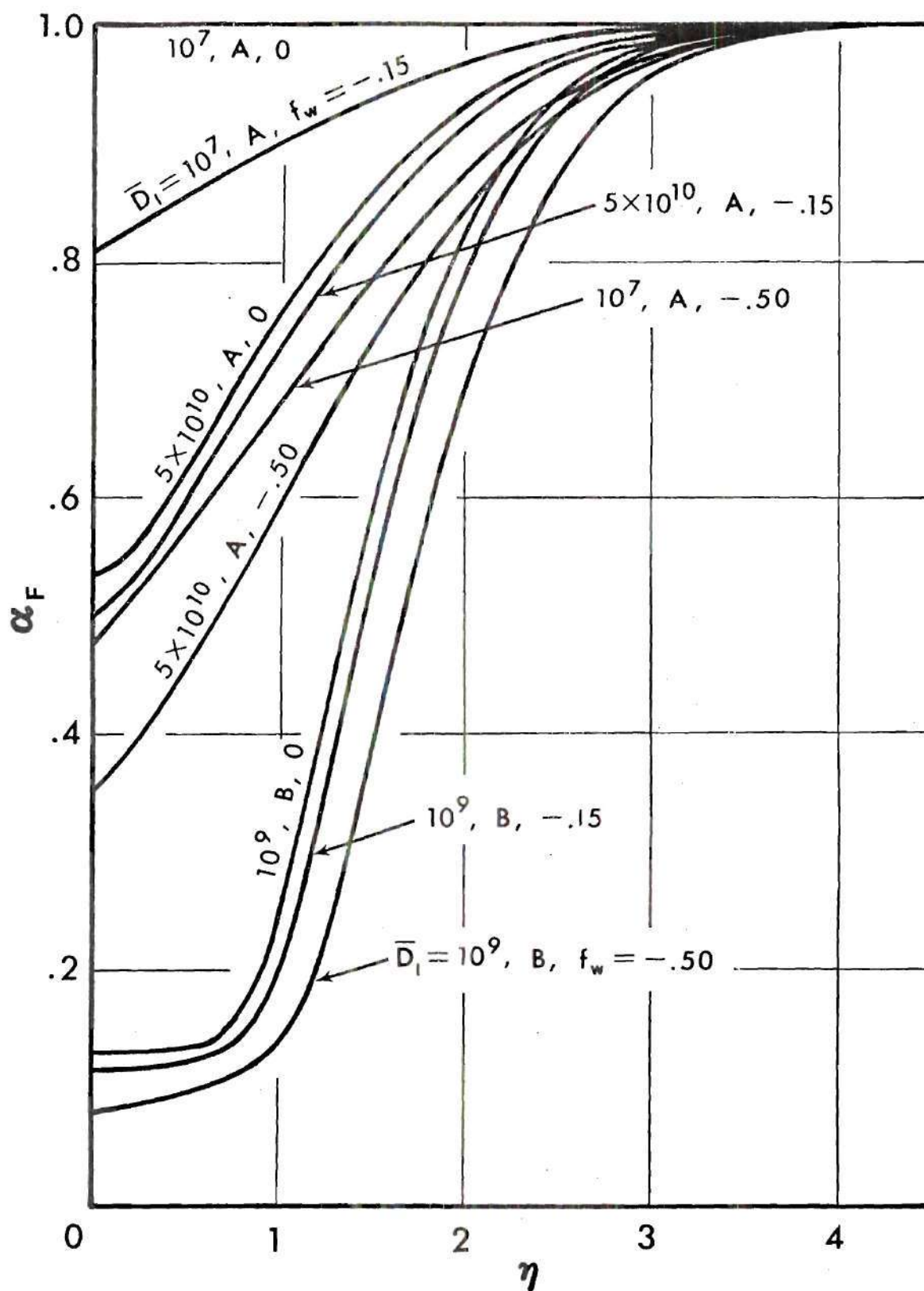


Figure 7. Comparison of Fuel Concentration Profiles at Specified Damköhler Numbers and Inert Gas Injection Rates

### 5.1.6. Temperature Distribution

The injection rate of the inert gas has very little influence on the maximum temperatures of the profiles as shown in Figure 8. Its significant effect on temperature profiles is primarily on the location of the maximum temperatures. With  $\bar{D}_I$  at  $10^9$  in branch B, the profiles for both injection rate of  $-0.05$  and  $-0.5$  have approximately the maximum value of  $4.5$ . The maximum occurs at  $\eta = 0.87$  for  $f_w = -0.05$  and at  $\eta = 1.1$  for  $f_w = -0.5$ . The reason that maximum temperature occurs further away from the wall is due to the fact that reaction zone is closer to the wall when injection rate of the inert gas is lower in branch B. While in branch A, since there is no reaction occurring, the maximum temperature is the same as the surface temperature at the wall through mixing.

The maximum temperature is higher in branch B due to the higher reaction rate.

### 5.1.7. Heat Transfer Rate Dependence on $f_w$

The dependence of the heat transfer rate on inert gas injection rate  $f_w$  varies through the flow transition from "equilibrium" to "frozen." It is well illustrated as in Figure 9. As mentioned in Section 5.1.3., injection of inert gas slows the heat transfer rate in both branches A and B. At the region near the characteristic first Damköhler number, the heat transfer rate is approximately constant.

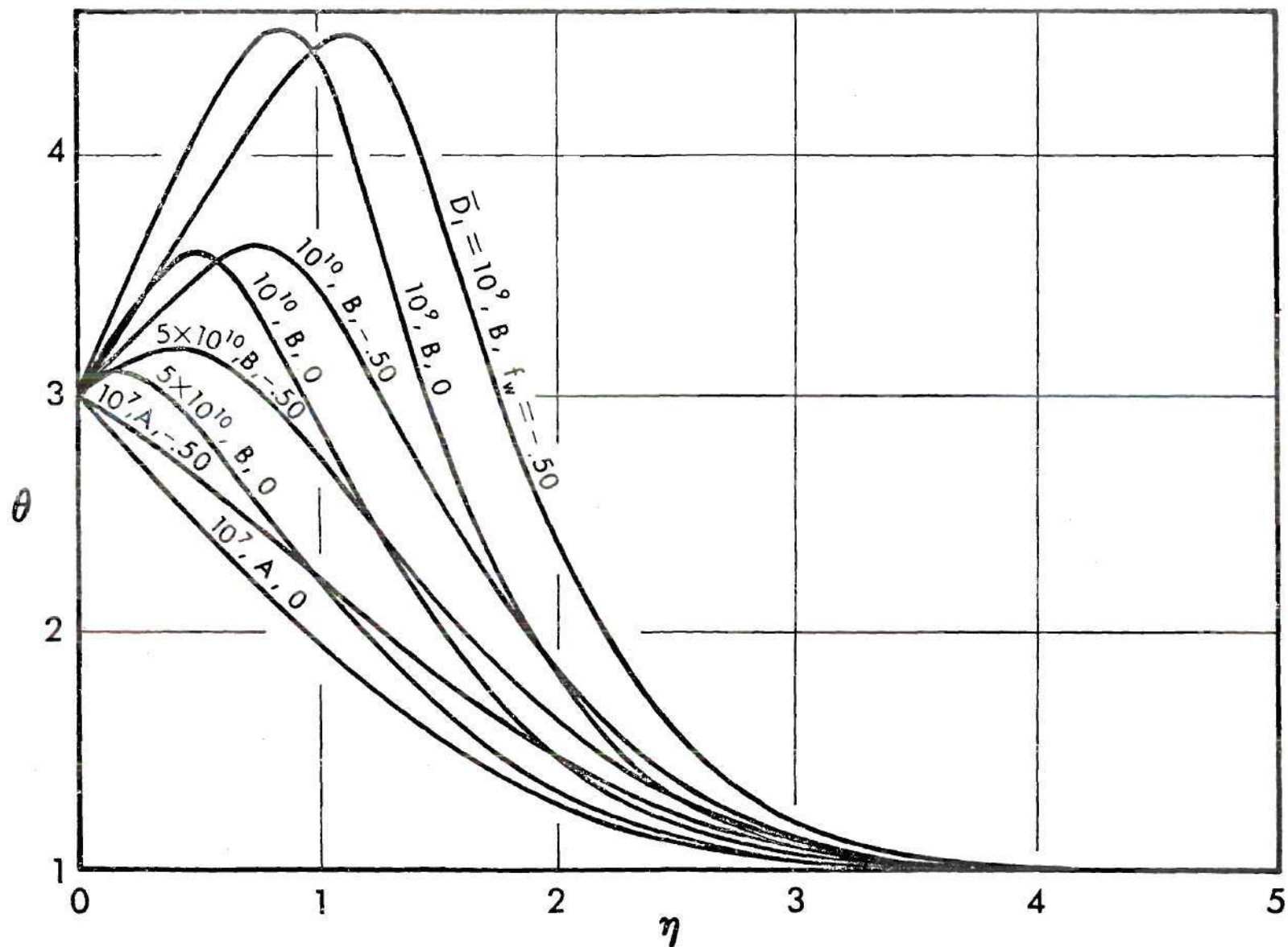


Figure 8. Comparison of Temperature Profiles at Specified Damköhler Numbers and Inert Gas Injection Rates

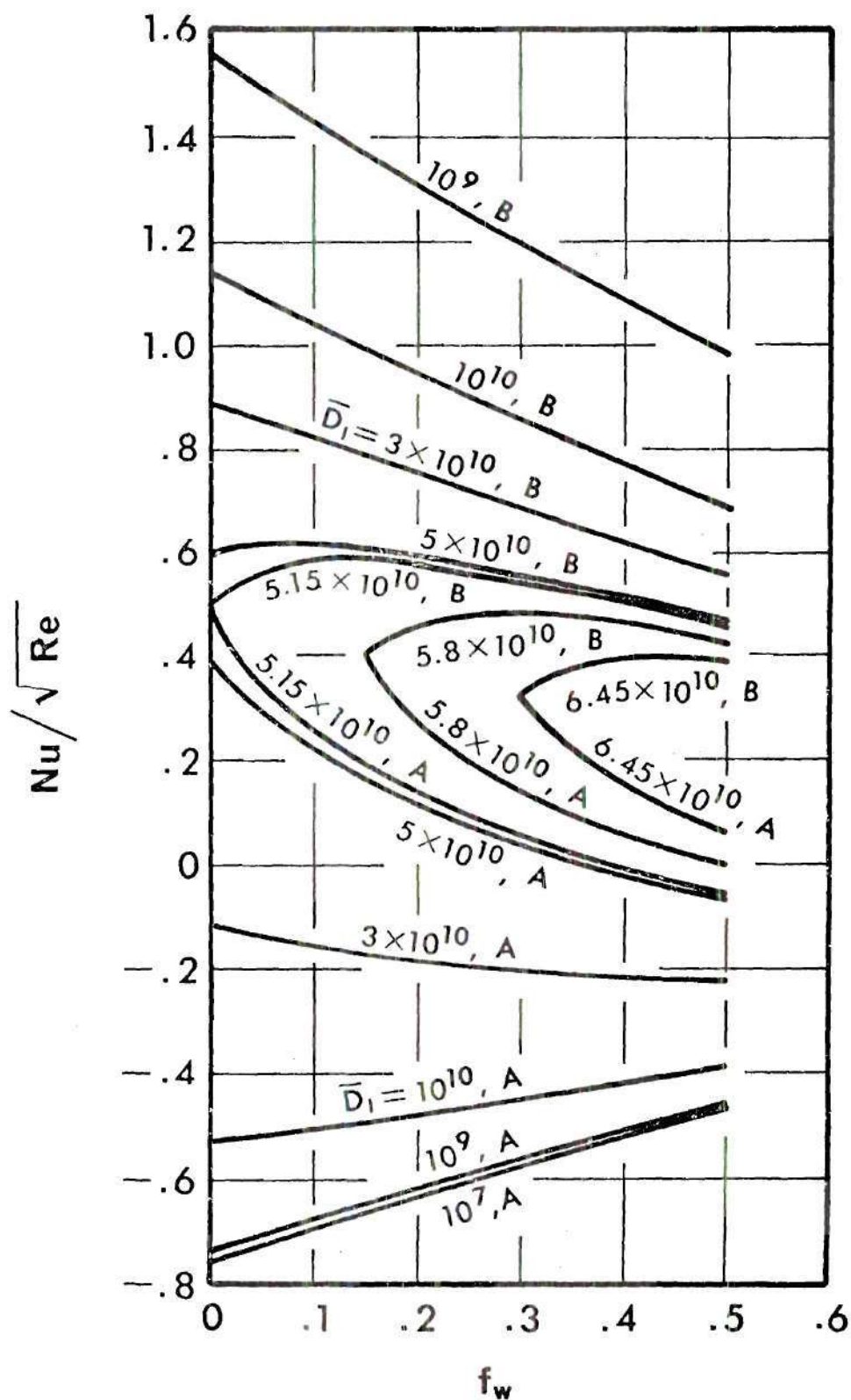


Figure 9. The Effect of Inert Gas Injection on the Surface Heat Transfer



### 5.1.8. Dependence of $\bar{D}_{I,i}$ on $f_w$

The dependence of the characteristic first Damköhler number of ignition  $\bar{D}_{I,i}$  on inert gas injection rate  $f_w$  is shown in Figure 10.  $\bar{D}_{I,i}$  increases linearly with  $f_w$ . It starts at  $5.15 \times 10^{10}$  when there is no injection at  $\theta_w = 3$ . It increases at the rate of approximately  $4.3 \times 10^{10}$  per each unit of  $f_w$ . The injection of the inert gas slows down the ignition as mentioned before due to the dilution of the mixture. The values of  $\bar{D}_{I,i}$  corresponding to different  $f_w$ 's are also tabulated in Table 2.

## 5.2. Results of the Opposed-Jet Case

### 5.2.1. Ignition Characteristics

Since the stagnation plane in the opposed-jet case varies its absolute location at different first Damköhler numbers, it is unreasonable to plot the fluid properties at this location versus its corresponding  $\bar{D}_I$ . However, the maximum temperature at each  $\bar{D}_I$  is an absolute and unique value without reference to the stagnation plane location and coordinate system. Therefore, the coordinates of  $\theta_{\max}$  and  $\bar{D}_I$  have been selected for investigation of ignition characteristics of opposed-jet.

The relationship between  $\theta_{\max}$  and  $\bar{D}_I$  is shown in Figure 11. The curve can be divided into three regions. In branch A, where frozen flow phenomenon is more significant, the temperature does not exceed the inert gas temperature.



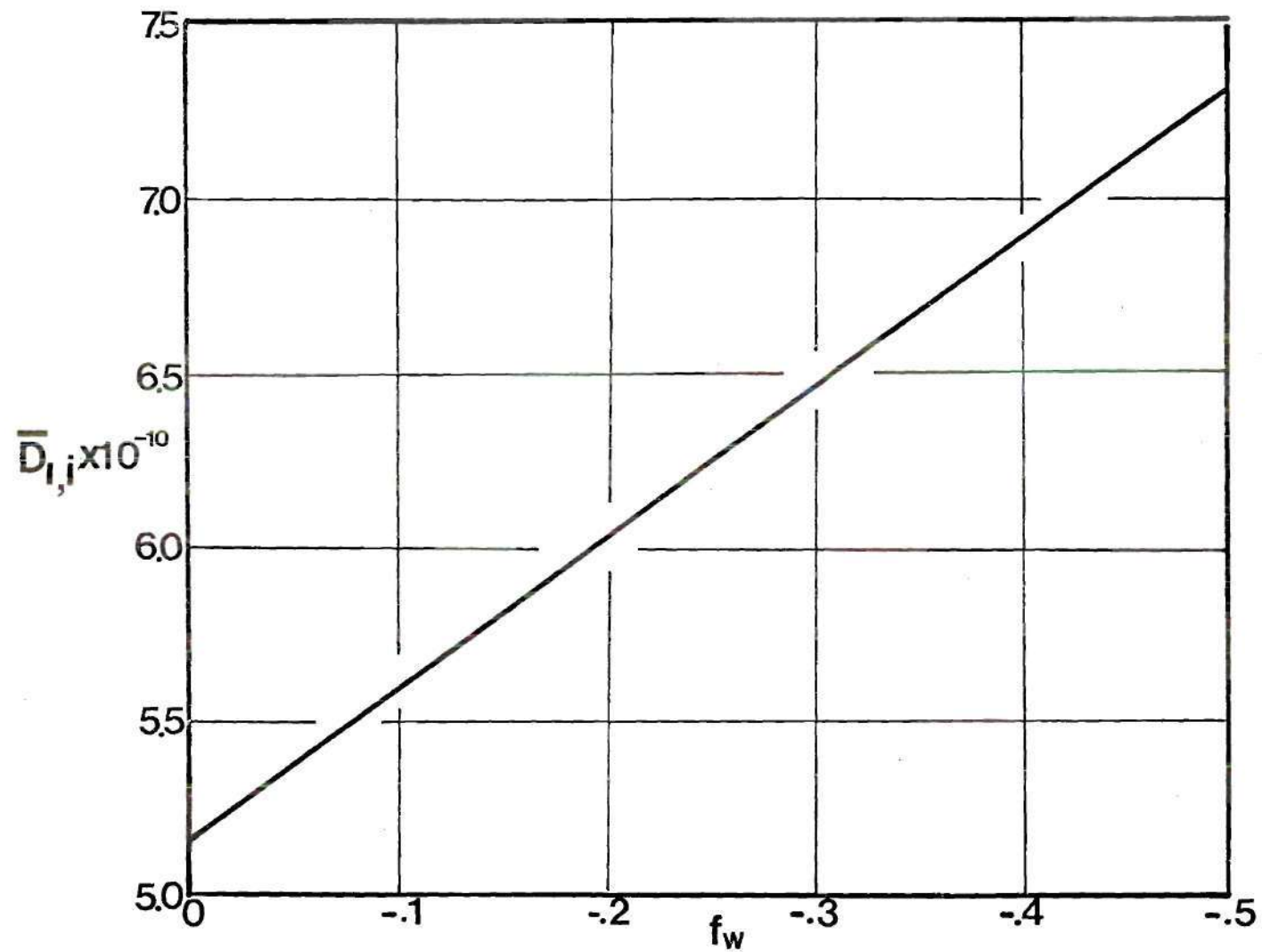


Figure 10. The Effect of Inert Gas Injection on the Ignition First Damköhler Number in the Impinging Jet

Table 2. Critical Ignition Damköhler Numbers at Different  $f_w$ 

$f_w$	$\bar{D}_{I,i}$
0	$5.15 \times 10^{10}$
-.15	$5.80 \times 10^{10}$
-.30	$6.45 \times 10^{10}$
-.50	$7.30 \times 10^{10}$

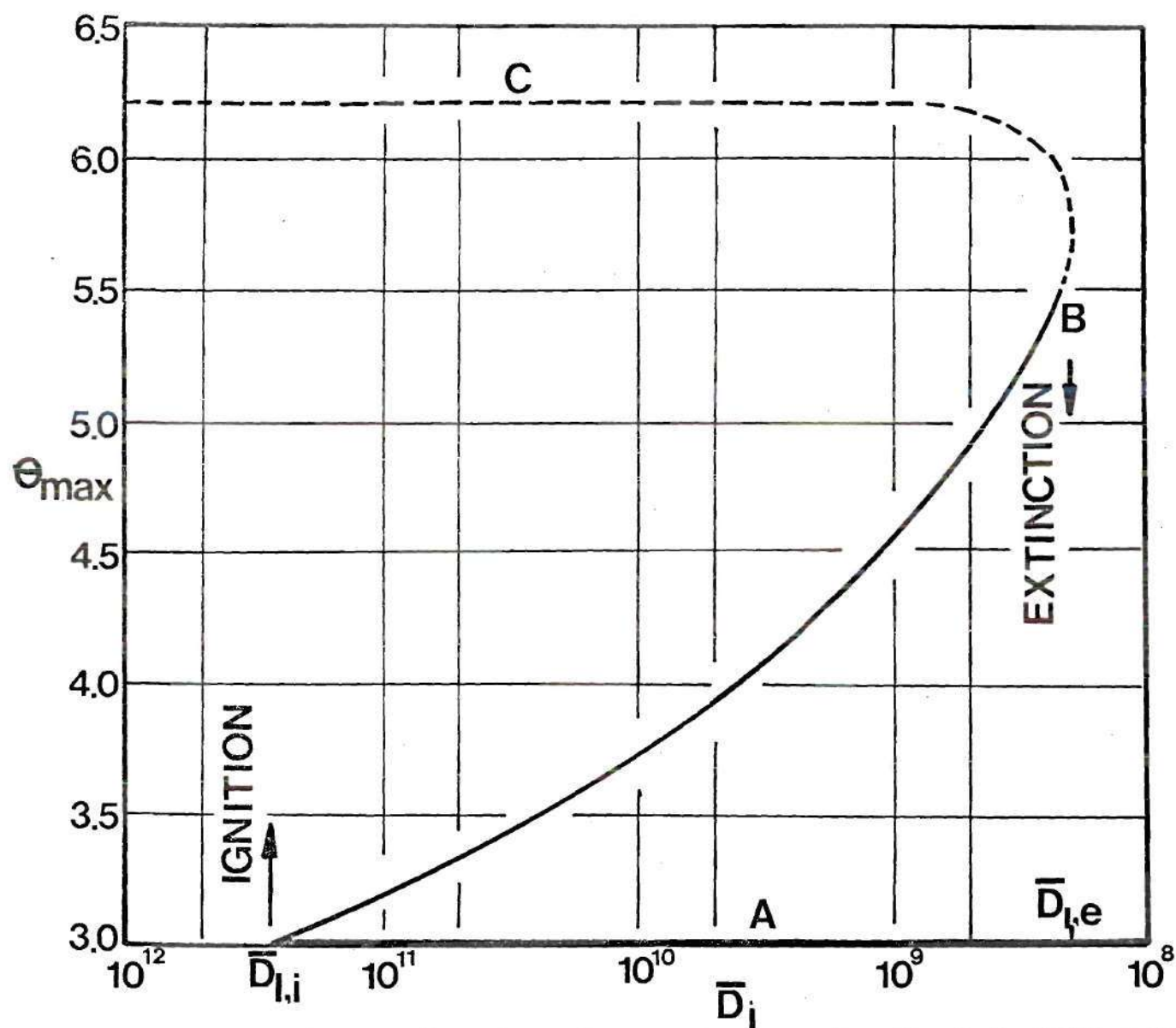


Figure 11. Dependence of Maximum Temperature on the First Damköhler Number in the Opposed-Jet Case,  $\theta_{-\infty} = 3.0$

Therefore, the maximum temperature remains constant. As the flow reaches the transition region in branch B and moves towards the "equilibrium" branch C, a reaction zone is formed near the interface. The exothermic reaction increases the maximum temperature above the inert gas free stream temperature. The value of the maximum temperature depends on the degree of completion of the reaction and it increases as more reaction takes place.

As the flow goes from frozen to equilibrium through the transition as shown in Figure 11, there exists a maximum value for  $\bar{D}_I$ . This  $\bar{D}_I$  is the characteristic first Damköhler number for ignition  $\bar{D}_{I,i}$ , where ignition occurs. Beyond  $\bar{D}_{I,i}$  equilibrium (branch C, dash line) is reached and ignition takes place. In branch C, the chemical rate of reaction is so fast that the flow is in equilibrium all the time. The maximum temperature also remains constant in this branch to form an upper bound for the fluid temperature. The study of this branch, however, is not in the scope of the present dissertation. The result is only predicted.

#### 5.2.2. Velocity Distribution

The velocity distribution for the opposed-jet case is shown in Figure 12. The  $\eta = 0$  plane is taken to be at  $f = 0$ , the stagnation plane, where no fluid would flow across the plane. On one side of the plane is the inert gas with a higher temperature ( $\theta_\infty = 3$ ) and a higher free stream velocity ( $f' = 3^{1/2}$ ). On the other side of the plane is a

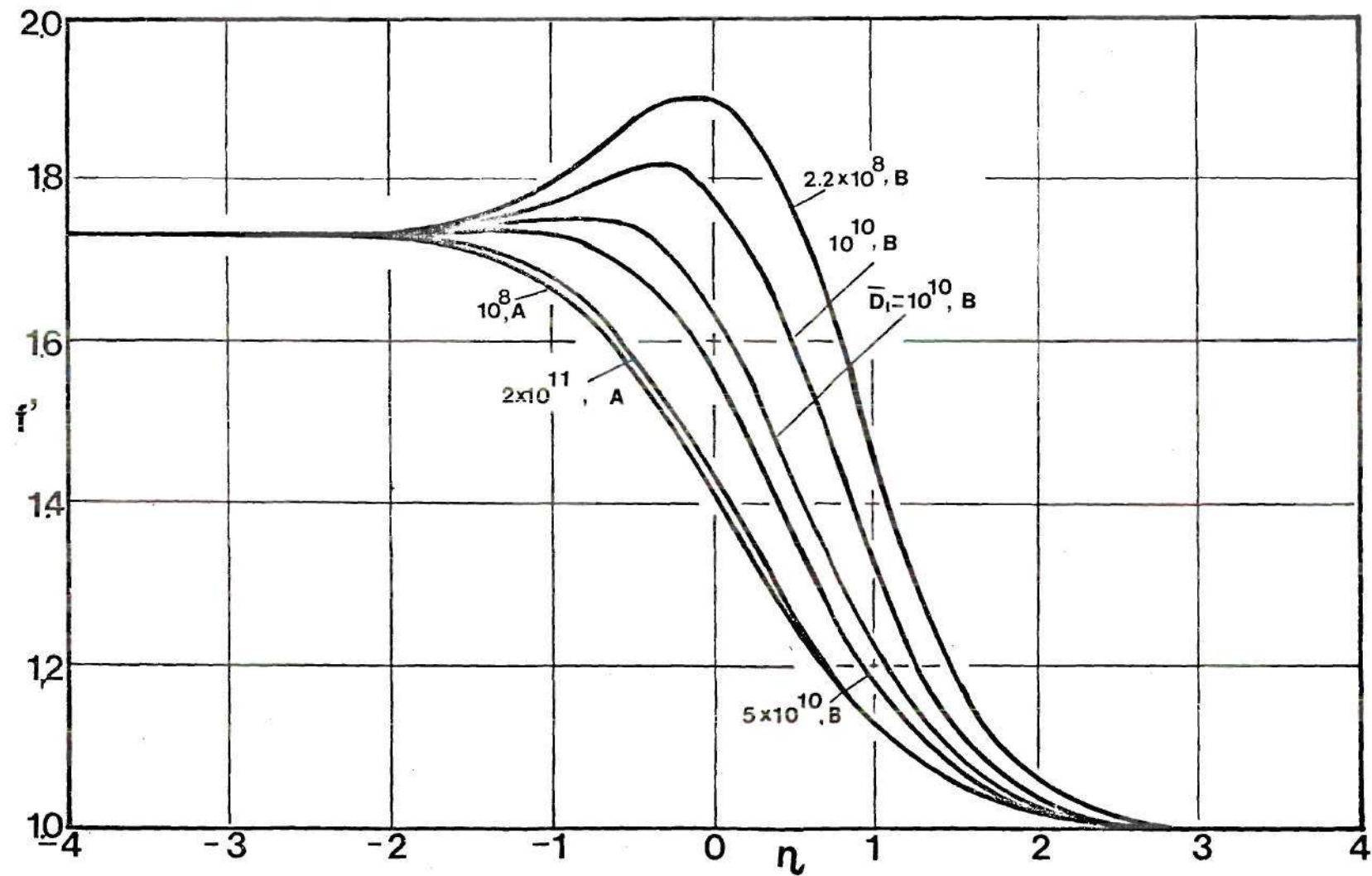


Figure 12. Comparison of Velocity Profiles at Specified Damköhler Number in the Opposed-Jet Case,  $\theta_{-\infty} = 3.0$



combustible mixture with a lower temperature ( $\theta_{\infty} = 1$ ) and unity velocity. The combustible mixture is at the stoichiometric composition. All velocity profiles must satisfy asymptotically the free stream velocities from both streams of the opposed flow.

In branch B, where there is reaction occurring, a maximum velocity which is higher than either one of the free stream velocities is reached due to the sudden decrease of the density in the reaction zone. It decreases towards unity on the combustible mixture side and towards  $3^{1/2}$  on the inert gas side. In branch A, the velocity is always between the limits of unity and  $3^{1/2}$ . Since the flow is frozen and there is no chemical reaction occurring, the velocity can never be higher than the inert gas free stream velocity.

#### 5.2.3. Fuel Concentration Profiles

All the fuel concentration profiles start at zero at the inert gas free stream since there is no fuel existing on that side of the opposed flow region. They all approach asymptotically to unity at the combustible mixture free stream side. In branch A, due to the lack of a chemical reaction, the fuel is preserved. Therefore, the fuel concentration reaches unity faster. On the other hand, in branch B, the fuel is used in the reaction to form products. Therefore,  $\alpha_F$  reaches unity with a steeper gradient. These results are shown in Figure 13.

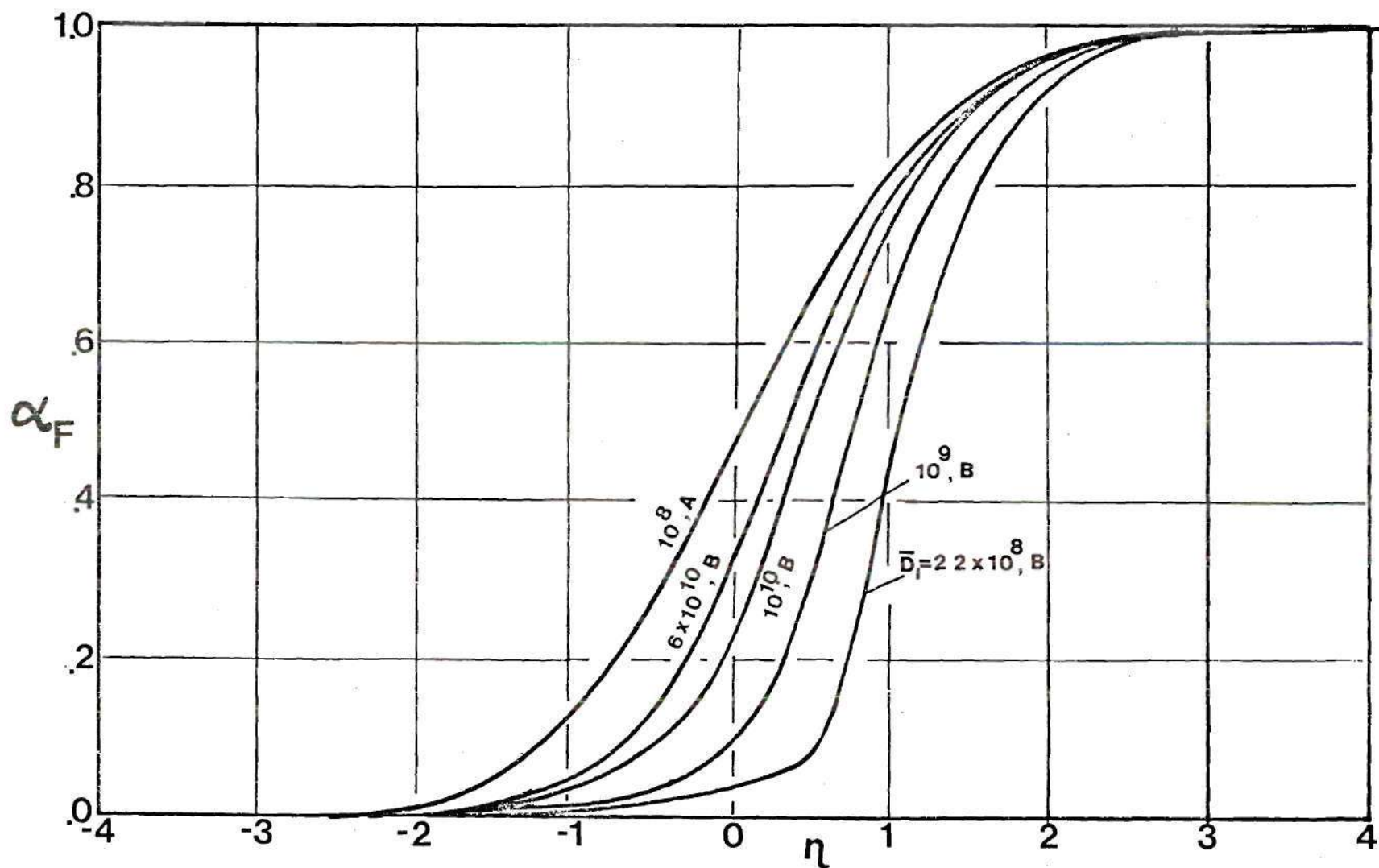


Figure 13. Comparison of Fuel Concentration Profiles at Specified Damköhler Number in the Opposed-Jet Case,  $\theta_{-\infty} = 3.0$

#### 5.2.4. Temperature Distribution

The temperature distributions shown in Figure 14 have similar profiles to the velocity profiles presented earlier. The similarity in profiles is reasonable with the consideration of the relationship between velocity, temperature, and density.

The intense reaction taking place in the flow specified along branch B establishes the higher temperature shown in Figure 12. In contrast, in branch A, the temperature can never be higher than the inert gas free stream temperature. The maximum temperature shifts from left to right across the  $\eta = 0$  plane. In branch A, where the flow is frozen and the temperature can never be more than the inert gas free stream temperature, the maximum temperature occurs at the inert gas free stream side. As the flow goes through the transition towards "equilibrium," chemical reaction occurs. A reaction zone is formed near the stagnation plane. It is first close to the inert gas free stream as the reaction rate is low. As the chemical reaction becomes more intense, the reaction zone shifts away across the stagnation plane and into the combustible mixture side.

#### 5.3. Generalized Ignition-Extinction Characteristics

Due to the lengthy computation required and due to the similar nature between extinction and ignition characteristics, the extinction characteristics have not been

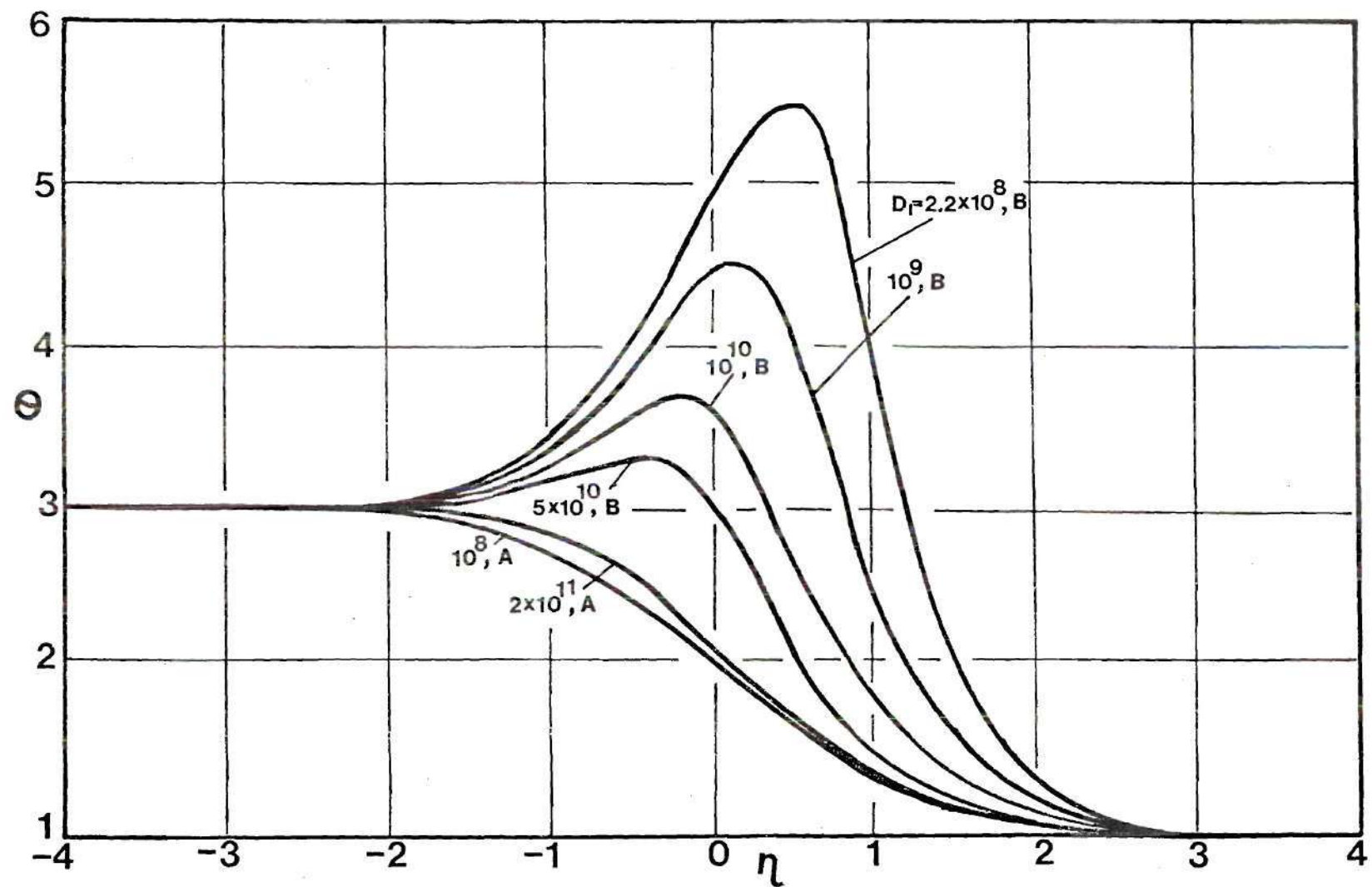


Figure 14. Comparison of Temperature Profiles at Specified Damköhler Number in Opposed-Jet Case,  $\theta_{\infty} = 3.0$



considered in this dissertation. However, a look at the overall ignition-extinction characteristics of a combustible mixture when it interacts with a hot surface or a hot gas is still necessary to provide a physical understanding of the results presented in the previous sections.

A generalized ignition-extinction curve is shown in Figure 15. This curve is similar to those presented in Figure 5 except that it extends the range of the calculations. The curve can be divided into three branches. The branches are separated by two critical values of the first Damköhler number specified as  $\bar{D}_{I,i}$  and  $\bar{D}_{I,e}$ . On branch A of the curve, no reaction or minimal reaction occurs. Therefore, for a range of values of  $\bar{D}_I$  up to  $\bar{D}_{I,i}$ , the quantity  $Nu/(Re)^{1/2}$  is independent of the first Damköhler number. This complies with the familiar Nusselt-Reynolds type equation for nonreactive heat transfer rate,  $Nu/(Re)^{1/2} = \phi(Pr)$ . On the other hand, for branch C, although the parameter  $Nu/(Re)^{1/2}$  is independent of  $\bar{D}_I$ , it is very much dependent on the injection rate  $f_w$ . Intense reaction takes place on this branch. Between branches A and C, a transition region is established which is designated in the figure as branch B.

Although a stability analysis was not carried out for this dissertation, it can be qualitatively studied through the following physical phenomena. If a combustible mixture is initially identified by a value of  $\bar{D}_I < \bar{D}_{I,e}$  (in frozen



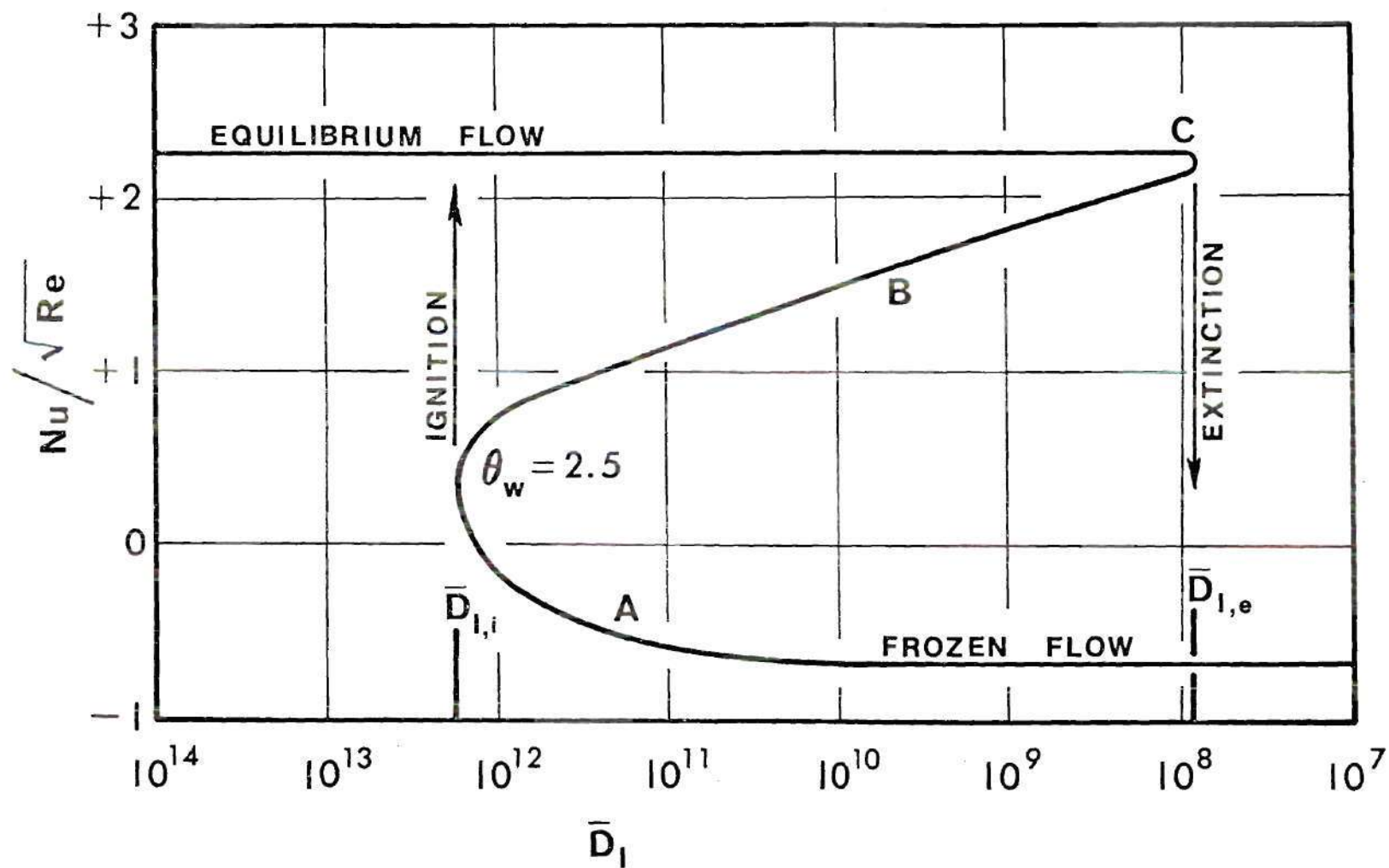


Figure 15. Ignition and Extinction Characteristics of a Stagnation Point Flow

flow), and this Damköhler number,  $\bar{D}_I$ , is increased (by decreasing the free stream velocity of the mixture) to bring the mixture to the region  $\bar{D}_{I,e} < \bar{D}_I < \bar{D}_{I,i}$ , then its surface heat transfer will be given by its value on branch A. If the Damköhler number is further increased until it reaches the value  $\bar{D}_{I,i}$ , a step jump to the equilibrium flow, branch C, occurs. Physically this constitutes ignition of the combustible mixture. Similarly, given a mixture which is burning under equilibrium conditions and it is initially identified by a  $\bar{D}_I > \bar{D}_{I,i}$ , this  $\bar{D}_I$  is decreased (by increasing the free-stream velocity of the premixed combustibles to bring the mixture to the region  $\bar{D}_{I,e} < \bar{D}_I < \bar{D}_{I,i}$ , then its surface heat transfer will be given by its value on branch C. If  $\bar{D}_I$  is further decreased until it reaches the value  $\bar{D}_{I,e}$ , a step jump to the frozen flow branch, branch A, occurs.

Physically this constitutes extinction for the burning mixture. Solution of the system governing equations established values between the frozen flow and the equilibrium flow branches. However, based on the above discussion it is apparent that it will be very difficult, if at all possible, to operate a physical system under the conditions designated by branch B. Consequently, branches A and C represent conditions for a physically stable system, while branch B represents a physically unstable system.

## CHAPTER VI

## CONCLUSIONS

A theoretical study of the steady-state theory of ignition of a premixed combustible gas mixture by a hot inert gas in opposed flow has been made. Based on boundary-layer approximations and similarity analysis, a general ignition equation was developed which relates the injection rate in the impinging jet case and the inert gas free stream temperature in the opposed-jet case to appropriate dimensionless parameters of the reactive flow. Of these parameters, two are of primary importance in describing the ignition characteristics of the systems: (a) the first Damköhler number  $\bar{D}_I$  which represents a measure of residence time of a fluid particle in the reaction zone relative to the chemical time, and (b) the Nusselt number  $Nu$  which represents the magnitude of the heat transfer at the gas-solid interface, and the maximum temperature in the reaction zone of the opposed-jet which represents the intensity of reactions between the streams.

The results which were plotted with the first Damköhler number as the independent parameter established the existence of a critical value of this parameter which is defined as the Ignition First Damköhler Number,  $\bar{D}_{I,i}$ .

In the case of  $\bar{D}_I > \bar{D}_{I,i}$ , the flow is always in equilibrium. For  $\bar{D}_{I,e} < \bar{D}_I < \bar{D}_{I,i}$ , the flow is multivalued. It can be in equilibrium, in frozen or in the transition region. For  $\bar{D}_I < \bar{D}_{I,e}$ , the Extinction First Damköhler Number, the flow is always "frozen," where no reaction occurs.

The results of the two cases shows the interaction of a hot inert gas with a cold premixed combustible mixture in opposed flow and establishes the conditions of ignition. The compressibility of the flow was considered in the analysis in obtaining a more exact solution. The numerical techniques utilized in reaching the present solution are efficient even for this complex problem.

## CHAPTER VII

### RECOMMENDATIONS

This study has dealt largely with the injection rate on the influence of ignition characteristics of an impinging jet, and the development of a numerical technique to deal with this type of problem. Several things are recommended for more extensive studies.

First of all, the temperature ratio of the two streams in the opposed-jet case can be varied to study its effects on ignition characteristics.

Secondly, an extinction first Damköhler number,  $\bar{D}_{I,e}$ , can be sought in each case to study the extinction characteristics.

Thirdly, an unmixed fuel and oxidizer opposed flow case can also be studied for its ignition and extinction characteristics.

The continuation of this study with the above mentioned extended features should make the results more interesting.



## REFERENCES

1. Lees, L., "Laminar Heat Transfer Over Blunt-Nosed Bodies at Hypersonic Flight Speeds," Jet Propulsion, Vol. 26, 1956, pp. 259-268.
2. Fay, J. A. and Riddell, F. R., "Theory of Stagnation Point Heat Transfer in Dissociated Air," Journal of the Aeronautical Sciences, Vol. 25, No. 2, 1958, pp. 73-85.
3. Fendell, F. E., "Ignition and Extinction in Combustion of Initially Unmixed Reactants," Journal of Fluid Mechanics, Vol. 21, Part 2, 1965, pp. 281-303.
4. Chambre, P. L., "On the Ignition of a Moving Combustible Gas Stream," Journal of Chemical Physics, Vol. 25, 1955, pp. 417-421.
5. Sharma, O. P. and Sirignano, W. A., "Ignition of a Stagnation Point Flow by a Hot Body," Combustion Science and Technology, Vol. 1, 1969, pp. 95-104.
6. Alkidas, A. and Durbetaki, P., "Ignition Characteristics of a Stagnation Point Combustible Mixture," Combustion Science and Technology, Vol. 3, 1971, pp. 187-194.
7. Alkidas, A. and Durbetaki, P., "A Simplified Model for Stagnation Heat Transfer and Ignition of a Gaseous Mixture," Transactions of the ASME, Journal of Heat Transfer, Vol. 95, 1973, pp. 564-566.
8. Alkidas, A. and Durbetaki, P., "Stagnation-Point Heat Transfer: The Effect of the First Damköhler Similarity Parameter," Transactions of the ASME, Journal of Heat Transfer, Vol. 94, 1972, pp. 410-414.
9. Alkidas, A. and Durbetaki, P., "Ignition of a Gaseous Mixture by a Heated Surface," Combustion Science and Technology, Vol. 7, 1973, pp. 135-140.
10. Smith, H. W., Schmitz, R. A. and Ladd, R. G., "Combustion of a Premixed System in Stagnation Flow--I. Theoretical," Combustion Science and Technology, Vol. 4, 1971, pp. 131-142.

11. Spalding, D. B., "Theory of Mixing and Chemical Reaction in the Opposed-Jet Diffusion Flame," ARS Journal, Volume 31, 1961, pp. 763-771.
12. Jain, V. K. and Mukunda, H. S., "On the Ignition and Extinction Problems in Forced Convection Systems," International Journal of Heat and Mass Transfer, Vol. 11, 1967, pp. 491-508.
13. Marathe, A. G. and Jain, V. K., "Some Studies on Opposed-Jet Diffusion Flame Considering General Lewis Number," Combustion Science and Technology, Vol. 6, 1972, pp. 151-157.
14. von Karman, Th. and Millan, G., Fourth International Symposium on Combustion, Williams and Wilkins Co., Baltimore, 1953, pp. 173-177.
15. Marble, F. E. and Adamson, T. C., Jr., "Ignition and Combustion in a Laminar Mixing Zone," Jet Propulsion, Vol. 24, 1954, p. 85.
16. Williams, F. A., Combustion Theory, Addison-Wesley Publishing Co., Inc., 1965.
17. Tsuji, H. and Yamaoka, I., "The Counterflow Diffusion Flame in the Forward Stagnation Region of a Porous Cylinder," Eleventh Symposium (International) on Combustion, The Combustion Institute, Pittsburgh, Pa., 1966, pp. 979-984.
18. Tsuji, H. and Yamaoka, I., "The Structure of Counterflow Diffusion Flames in the Forward Stagnation Region of a Porous Cylinder," Twelfth Symposium (International) on Combustion, The Combustion Institute, Pittsburgh, Pa., 1969, pp. 997-1005.
19. Tsuji, H. and Yamaoka, I., "Structure Analysis of Counterflow Diffusion Flames in the Forward Stagnation Region of a Porous Cylinder," Thirteenth Symposium (International) on Combustion, The Combustion Institute, Pittsburgh, Pa., 1971, p. 723.
20. Wu, P. and Libby, P. A., "Further Results on the Stagnation Point Boundary Layer with Hydrogen Injection," Combustion Science and Technology, Vol. 6, 1972, pp. 159-168.

21. Jones, F. L., Becker, P. M. and Heinsohn, R. J., "A Mathematical Model of the Opposed-Jet Diffusion Flame: Effect of an Electric Field on Concentration and Temperature Profiles," Combustion and Flame, Vol. 19, 1972, pp. 351-362.
22. Anagnostou, E. and Potter, A. E., Jr., "Flame Strength of Propane-Air Flames at Low Pressure in Turbulent Flow," Ninth Symposium (International) on Combustion, Academic Press, New York, 1963, pp. 1-6.
23. Chung, P. M., Fendell, F. E. and Holt, J. F., "Nonequilibrium Anomalies in the Development of Diffusion Flames," AIAA Journal, Vol. 4, 1966, pp. 1020-1025.
24. Nachsteim, D. R. and Swigert, P., Satisfaction of Asymptotic Boundary Condition in Numerical Solution of Systems of Nonlinear Equations of Boundary-Layer Type, NASA Technical Notes, No. TN D-3004, 1965.
25. Fox, L., ed., Numerical Solution of Ordinary and Partial Differential Equations, Pergamon Press, 1962, Chapter 5.
26. Radbill, J. R., "Application of Quasilinearization to Boundary-Layer Equations," AIAA Journal, Vol. 2, No. 10, 1964, pp. 1860-1862.
27. Hartree, D. R., Numerical Analysis, Clarendon Press, Oxford, 1952, pp. 143-144.
28. Hartree, D. R., "On an Equation Occurring in Falkner and Skan's Approximate Treatment of the Equations of the Boundary Layer," Proceedings Cambridge Phil. Society, Vol. 33, Part 2, 1937, pp. 223-239.



## OTHER REFERENCES

- Emmons, H. W., "Plenary Lecture: Fluid Mechanics and Combustion," Thirteenth Symposium (International) on Combustion, The Combustion Institute, Pittsburgh, Pa., 1971, pp. 1-18.
- Emmons, H. W. and Mukunda, H. S., "Tabulation of the Blasius Function with Blowing and Suction," Aeronautical Research Council, Current Paper, No. 157, 1954.
- Fang, M., Schnitz, R. A. and Ladd, R. G., "Combustion of a Premixed System in Stagnation Flow--II. Experiments with Carbon Monoxide Oxidation," Combustion Science and Technology, Vol. 4, 1971, pp. 143-148.
- Goh, S. Y. and Ma, A. S. C., "A Theoretical Investigation Into the Ignition of Explosive Environment by a Hot, Laminar, Round, Inert Gaseous Jet," Heat Transfer 1970, Vol. III, Fourth International Heat Transfer Conference, Paris-Versailles, Elsevier Publishing Company, Amsterdam, 1970, F. C.8.1.
- Goldstein, S., ed., Modern Developments in Fluid Mechanics, Vol. 1, Dover Publications, New York, 1965.
- Hartnett, J. P. and Eckert, E. R. G., "Mass-Transfer Cooling in a Laminar Boundary-Layer with Constant Fluid Properties," Transactions of the ASME, 1957, pp. 247-254.
- Lee, L., "Convective Heat Transfer with Mass Addition and Chemical Reactions," Combustion and Propulsion, Third AGARD Colloquium, Pergamon Press, Oxford, 1958, pp. 451-498.
- Pai, Shih-i, Fluid Dynamics of Jets, D. van Nostrand Co., Princeton, 1954.
- Schlichting, H., Boundary Layer Theory, McGraw-Hill, New York, 1960.
- Weinberg, F. J. and Wilson, J. R., "An Optical Study of Pre-Ignition Heat Release," Proceedings of Royal Society, London, A.314, 1970, pp. 175-193.

## VITA

Heng-Wai Hsu was born May 4, 1943, in Shanghai, China. He entered Georgia Tech as a freshman in the School of Mechanical Engineering in 1963, and obtained his BME degree in 1967. He chose to stay at Georgia Tech to continue his graduate study in the field of thermal sciences. He worked part-time as a laboratory assistant during his graduate study. He is a member of the Pi Tau Sigma Society.

Mr. Hsu is married to the former Miss Tsai of Taipei, Taiwan.